

Reply to the Comments by Reviewer #1 on GMD-2024-114

“ Evaluation of Dust Emission and Land Surface Schemes in Predicting a Mega Asian Dust Storm over South Korea Using WRF-Chem (v4.3.3)”

By Ji Won Yoon, Seungyeon Lee, Ebony Lee, and Seon Ki Park

This manuscript examines the performance of 20 combinations of WRF-Chem dust aerosol parameterizations and land-surface schemes in reproducing a mega Asian Dust Storm (ADS) from March 2021. The validation study is highly specific to a single numerical modeling system and individual event, so the novelty of this study and its broader impact on the wider atmospheric sciences is limited. However, I recognize that verification studies like this are sometimes important incremental steps within larger projects, and the results may nonetheless help guide the selection of appropriate dust physics settings among other researchers and practitioners in East Asia. The manuscript, though modest in its scope and potential scientific impact, is nonetheless well written and soundly conducted. I believe it could be accepted for publication pending the revisions suggested below.

→ We sincerely appreciate the reviewer's positive and valuable comments. We have carefully considered each comment and provided an item-by-item response below.

Overall Comment:

1. The manuscript computes both POD and FAR for several ACWS-relevant PM10 thresholds, and it emphasizes that these two scores need to be interpreted jointly. However, performance metrics such as the Critical Success Index (CSI) do exactly that. The manuscript would be strengthened by the addition of CSI, or a similar metric, that merges these two ideas into a single score. The CSI is easy to compute with the information already provided in the manuscript.

→ We believe the reviewer's comment is valid. According to the reviewer's comment, we have added the Critical Success Index (CSI) to Table 4. Additionally, we have included explanations of the basic concept of CSI and provided an analysis of the simulation results based on CSI in the manuscript.

(Original manuscript) Table 4

Table 4: POD and FAR values for each PM10 threshold across all scheme combinations. The bold numbers indicate POD greater than 0.5. The dashes '-' indicate POD and FAR values that cannot be calculated.

		> 80 µg m ⁻³		> 150 µg m ⁻³		≥ 300 µg m ⁻³		≥ 800 µg m ⁻³	
		POD	FAR	POD	FAR	POD	FAR	POD	FAR
GOCART	Noah	0.055	0.164	-	-	-	-	-	-
	RUC	0.097	0.221	-	-	-	-	-	-
	Noah-MP	0.114	0.120	-	-	-	-	-	-
	CLM4	0.079	0.298	0.002	0.500	-	-	-	-
AFWA	Noah	0.090	0.128	-	-	-	-	-	-
	RUC	0.223	0.256	0.027	0.063	-	-	-	-
	Noah-MP	0.126	0.103	-	-	-	-	-	-
	CLM4	0.110	0.264	0.007	0.333	-	-	-	-
UoC01	Noah	0.076	0.171	-	-	-	-	-	-
	RUC	0.516	0.401	0.251	0.305	0.057	0.048	-	-
	Noah-MP	0.138	0.073	-	-	-	-	-	-
	CLM4	0.918	0.297	0.758	0.351	0.448	0.325	0.034	0.727
UoC04	Noah	0.077	0.169	-	-	-	-	-	-
	RUC	0.544	0.407	0.282	0.331	0.075	0.037	-	-
	Noah-MP	0.152	0.093	-	-	-	-	-	-
	CLM4	0.928	0.310	0.799	0.378	0.520	0.320	0.069	0.714
UoC11	Noah	0.031	0.257	-	-	-	-	-	-
	RUC	0.149	0.225	-	-	-	-	-	-
	Noah-MP	0.060	0.138	-	-	-	-	-	-
	CLM4	0.071	0.298	0.002	0.500	-	-	-	-

(Revised manuscript) Table 4

Table 4: POD, FAR, and CSI values for each PM10 threshold across all scheme combinations. The bold numbers indicate that POD is greater than 0.5 and CSI is relatively higher compared to the others. The dashes '-' indicate POD, FAR, and CSI values that cannot be calculated.

		> 80 µg m ⁻³			> 150 µg m ⁻³			≥ 300 µg m ⁻³			≥ 800 µg m ⁻³		
		POD	FAR	CSI	POD	FAR	CSI	POD	FAR	CSI	POD	FAR	CSI
GO-CART	Noah	0.055	0.164	0.055	-	-	-	-	-	-	-	-	-
	RUC	0.097	0.221	0.095	-	-	-	-	-	-	-	-	-
	Noah-MP	0.114	0.120	0.112	-	-	-	-	-	-	-	-	-

	CLM4	0.079	0.298	0.077	0.002	0.500	0.002	-	-	-	-	-	-
AFWA	Noah	0.090	0.128	0.089	-	-	-	-	-	-	-	-	-
	RUC	0.223	0.256	0.207	0.027	0.063	0.027	-	-	-	-	-	-
	Noah-MP	0.126	0.103	0.124	-	-	-	-	-	-	-	-	-
	CLM4	0.110	0.264	0.106	0.007	0.333	0.007	-	-	-	-	-	-
UoC01	Noah	0.076	0.171	0.074	-	-	-	-	-	-	-	-	-
	RUC	0.516	0.401	0.383	0.251	0.305	0.226	0.057	0.048	0.057	-	-	-
	Noah-MP	0.138	0.073	0.136	-	-	-	-	-	-	-	-	-
	CLM4	0.918	0.297	0.661	0.758	0.351	0.537	0.448	0.325	0.369	0.034	0.727	0.032
UoC04	Noah	0.077	0.169	0.076	-	-	-	-	-	-	-	-	-
	RUC	0.544	0.407	0.396	0.282	0.331	0.247	0.075	0.037	0.074	-	-	-
	Noah-MP	0.152	0.093	0.150	-	-	-	-	-	-	-	-	-
	CLM4	0.928	0.310	0.655	0.799	0.378	0.538	0.520	0.320	0.418	0.069	0.714	0.059
UoC11	Noah	0.031	0.257	0.031	-	-	-	-	-	-	-	-	-
	RUC	0.149	0.225	0.143	-	-	-	-	-	-	-	-	-
	Noah-MP	0.060	0.138	0.059	-	-	-	-	-	-	-	-	-
	CLM4	0.071	0.298	0.069	0.002	0.500	0.002	-	-	-	-	-	-

(Original manuscript) Lines 296~301

Therefore, it is essential to consider FAR with POD to address these limitations. The formulas for POD and FAR are as follows:

$$POD = \frac{a}{a+c} \quad (10)$$

$$FAR = \frac{b}{b+d} \quad (11)$$

(Revised manuscript) Addition

Therefore, it is essential to consider FAR with POD to address these limitations. Additionally, the Critical Success Index (CSI) is an important metric used to evaluate the overall accuracy of forecasts. It measures the ratio of correctly forecast events to the total number of observed and forecast events, accounting for both ‘False Alarm’ and ‘Miss’ events. In other words, CSI addresses the limitations of POD and FAR by integrating both metrics, providing a clearer assessment of overall forecast performance. The CSI value ranges from 0 to 1, with values closer to 1 indicating higher forecast skill. CSI is particularly useful because it considers both over-forecasting and under-forecasting, showing

how accurate the forecast is. The formulas for POD, FAR, and CSI are as follows:

$$POD = \frac{a}{a+c} \quad (10)$$

$$FAR = \frac{b}{b+d} \quad (11)$$

$$CSI = \frac{a}{a+b+c} \quad (12)$$

(Original manuscript) Lines 413 ~ 414

Therefore, considering both POD and FAR, UoC04-CLM4 demonstrated the best performance, followed by UoC01-CLM4.

(Revised manuscript) Addition

Therefore, considering both POD and FAR, UoC04-CLM4 demonstrated the best performance, followed by UoC01-CLM4.

In addition to POD and FAR, CSI provides a comprehensive evaluation of forecast accuracy by accounting for correct predictions, false alarms, and missed events. The CSI values for all scheme combinations for each threshold are as follows: 1) At $80 \mu\text{g m}^{-3}$, UoC04-CLM4 and UoC01-CLM4 exhibited the highest CSI values of 0.655 and 0.661, respectively, while the other schemes had significantly lower values, mostly below 0.2, except for UoC04-RUC (0.396) and UoC01-RUC (0.383); 2) At $150 \mu\text{g m}^{-3}$, UoC04-CLM4 and UoC01-CLM4 demonstrated CSI values of 0.538 and 0.537, respectively, indicating higher prediction accuracy compared to other scheme combinations; 3) At $300 \mu\text{g m}^{-3}$, UoC04-CLM4 outperformed the other schemes with a CSI of 0.418. Although this was a comparatively lower value, it still demonstrated better performance compared to the other schemes, most of which showed poor or non-existent forecast skill; 4) At $800 \mu\text{g m}^{-3}$, only UoC01-CLM4 and UoC04-CLM4 were calculated only for CSI, but both showed very low values of 0.059 and 0.032, respectively. Overall, UoC04-CLM4 consistently maintained CSI values above 0.5 up to $300 \mu\text{g m}^{-3}$, showing the highest performance among all experiments.

2. The study references PM10 PCC values (Figure 6) and scatterplot relationships as “good” for some scheme combinations. However, visually, the observed-vs-simulated PM10 relationships appear quite weak. The PCCs for even the most skillful LSM-dust scheme combinations still only explain a relatively small fraction of the variance (~30% at most) if thought of as R^2 rather than R . The manuscript should clarify how the PCCs, even low ones, are indicating “good” performance.

→ We appreciate the reviewer giving us these valuable comments, which further improved the quality of the manuscript. Following the reviewer's comment, we acknowledge that the explanation suggesting good performance despite the low correlation for PM10 lacked clarity. The PCC value of the most skillful LSM-dust scheme combination for PM10 is lower compared to those of meteorological variables, such as 2m temperature and relative humidity. Therefore, for PM10, we think that the term "better" is more appropriate than "good" when comparing with other scheme combinations. Based on this, we have revised the manuscript as follows.

(Original manuscript) Lines 354~360

Fig. 6 shows PCC, RMSE, and MBE for all scheme combinations. Overall, UoC04-CLM4 showed the best performance, followed by UoC01-CLM4. The UoC04-RUC and UoC01-RUC also showed good performance compared to other scheme combinations. Conversely, the combinations of UoC01 and UoC04 with Noah and Noah-MP, as well as the combinations of GOCART, AFWA, and UoC11 with all land surface schemes, performed poorly. The detailed descriptions of the verification results are as follows: 1) For PCC (Fig. 6a), UoC04-CLM4 showed the highest value (0.61), indicating the best performance, followed by UoC01-CLM4 (0.60), UoC04-RUC (0.47), and UoC01-RUC (0.44). In all scheme combinations except for combinations of UoC04 and UoC01 with CLM4 and RUC, PCC was below 0.4, indicating very weak or almost no correlation; ~

(Revised manuscript)

Fig. 6 shows PCC, RMSE, and MBE for all scheme combinations. Overall, UoC04-CLM4 showed the best performance, followed by UoC01-CLM4. The UoC04-RUC and UoC01-RUC **also demonstrated relatively better** performance compared to other scheme combinations. Conversely, the combinations of UoC01 and UoC04 with Noah and Noah-MP, as well as the combinations of GOCART, AFWA, and UoC11 with all land surface schemes, **showed poor performance**. The detailed descriptions of the verification results are as follows: 1) For PCC (Fig. 6a), UoC04-CLM4 showed the highest value (0.61), **indicating a moderate correlation**, followed by UoC01-CLM4 (0.60), UoC04-RUC (0.47), and UoC01-

RUC (0.44) which also showed moderate correlations. In all other scheme combinations except for UoC04 and UoC01 with CLM4 and RUC, PCC was below 0.3, indicating a weak or almost no correlation; ~

※ Please refer to “Point 6” for the correlation strength criteria of the PCC.

(Original manuscript) Lines 376~386

Figure 7 shows a scatter diagram for CLM4-based combination---the land surface scheme that showed the best prediction performance when combined with UoC04 and UoC01 in the verification (see Fig. 6). The x-axis represents PM10 observations, while the y-axis indicated the predicted values of PM10 for each experiment. The red circles represent the predicted PM10 values corresponding to observations. The scheme combinations UoC04-CLM4 (Fig. 7c) and UoC01-CLM4 (Fig. 7d) showed similarly good performances while the other three combinations showed no correlations between observations and forecasts (Fig. 7a, b, and e): UoC04-CLM4---the best performance in verification---primarily showed overestimation for values below approximately $180 \mu\text{g m}^{-3}$ and wider dispersion with underestimation tendencies for values above $180 \mu\text{g m}^{-3}$.

(Revised manuscript)

Figure 7 shows a scatter diagram for the CLM4-based combination---the land surface scheme that demonstrated the best prediction performance when combined with UoC04 and UoC01 in the verification (see Fig. 6). The x-axis represents PM10 observations, while the y-axis indicates the **simulated** PM10 values for each experiment. The red circles represent the **simulated** PM10 values corresponding to the **observations**. In UoC04-CLM4 (Fig. 7c) and UoC01-CLM4 (Fig. 7d), the blue solid line shows that the trend between observed and simulated values generally increases positively compared to other scheme combinations. However, in UoC04-CLM4---which showed the best performance in the verification---the model primarily overestimates values below approximately $180 \mu\text{g m}^{-3}$ and exhibits wider dispersion with underestimation tendencies for values above $180 \mu\text{g m}^{-3}$. In contrast, the other three combinations (Fig. 7a, b, and e) showed little to no correlation between observations and simulations, with a wider spread of data. Therefore, UoC04-CLM4 showed relatively better performance compared to the other scheme combinations.

(Original manuscript) Supplement

Fig. S3 shows a scatter diagram for UoC04-based combination---the dust emission scheme that showed the best prediction performance when combined with CLM4 in the verification (see Fig. 6). As mentioned earlier, the UoC04-CLM4 combination exhibited the highest correlation, followed by UoC04-RUC. In contrast, the UoC04-Noah and UoC04-Noah-MP showed no linear correlation (Figs. S3a, and c).

(Revised manuscript)

Fig. S3 shows a scatter diagram for the UoC04-based combinations---the dust emission scheme that showed the best prediction performance when combined with CLM4 in the verification (see Fig. 6). The UoC04-CLM4 combination showed the highest correlation between observed and simulated values among the UoC04-based combinations. In contrast, UoC04-Noah and UoC04-Noah-MP demonstrated little to no correlation, suggesting very low prediction reliability.

Specific Comments:

1. Does this mean you wrote the output at 1-hr intervals? The integration timestep had to be much shorter than this.

→ We appreciate the reviewer for pointing this out. The previous explanation was unclear. We have revised the manuscript to clarify this point accordingly.

(Original manuscript) Line 166

We run WRF-Chem with a 1-hour interval from the occurrence of ADSs in the source region to their complete disappearance in South Korea, including a spin-up time of 72 hours; ~

(Revised manuscript)

We ran WRF-Chem, including a 72-hour spin-up time, from the occurrence of ADSs in the source region until their complete disappearance in South Korea, and the model output was saved at 1-hour intervals;

~

2. MAE is referenced as MBE throughout the rest of the manuscript. Please revise for consistency.

→ We sincerely appreciate your thoughtful review. We have carefully checked the entire manuscript

and corrected mention of MAE to MBE.

(Original manuscript) Line 281

;mean bias error (MAE) is the arithmetic average of ~

(Revised manuscript)

;mean bias error (MBE) is the arithmetic average of ~

3. 1.0 does not necessarily indicate a “perfect forecast.” It just indicates that all true events were successfully identified. The manuscript clarifies this in the following sentence, but “skillful” is more appropriate phrasing than “perfect.”

→ We appreciate your insightful comment. We agree that 1.0 indicates the successful identification of all true events, not a "perfect forecast". Based on your suggestion, I have revised "perfect" with "skillful".

(Original manuscript) Line 290

It ranges from 0 to 1, with 1 indicating a perfect forecast and ~

(Revised manuscript)

It ranges from 0 to 1, with 1 indicating a skillful forecast and ~

4. What is the basis of using 0.4 as the threshold for a “weak” correlation?

→ We appreciate the reviewer’s comment. After careful consideration, we realize that using 0.4 as a threshold for PCC was generalized without sufficient basis. Generally, interpretations of relationship strength may vary across disciplines (Turney et al., 2022). Therefore, we referred to the criteria used in air quality-related study (Cha et al, 2018).

Relationship strength:

- **Strong:** Values between ± 0.7 and ± 1 indicate a strong correlation.
- **Moderate:** Values between ± 0.3 and ± 0.7 indicate a moderate correlation.
- **Weak:** Values between ± 0.1 and ± 0.3 indicate a weak correlation.
- **No Correlation:** Values between 0 and ± 0.1 indicate negligible correlation.

※ Reference: Analysis of fine dust correlation between air quality and meteorological factors using SPSS (Cha et al, 2018)

Therefore, based on the above, we have revised the manuscript as follows.

(Revised manuscript) Figure 4

→ We adjusted the minimum value of the y-axis in the figure to 0.3 and modified the caption accordingly.

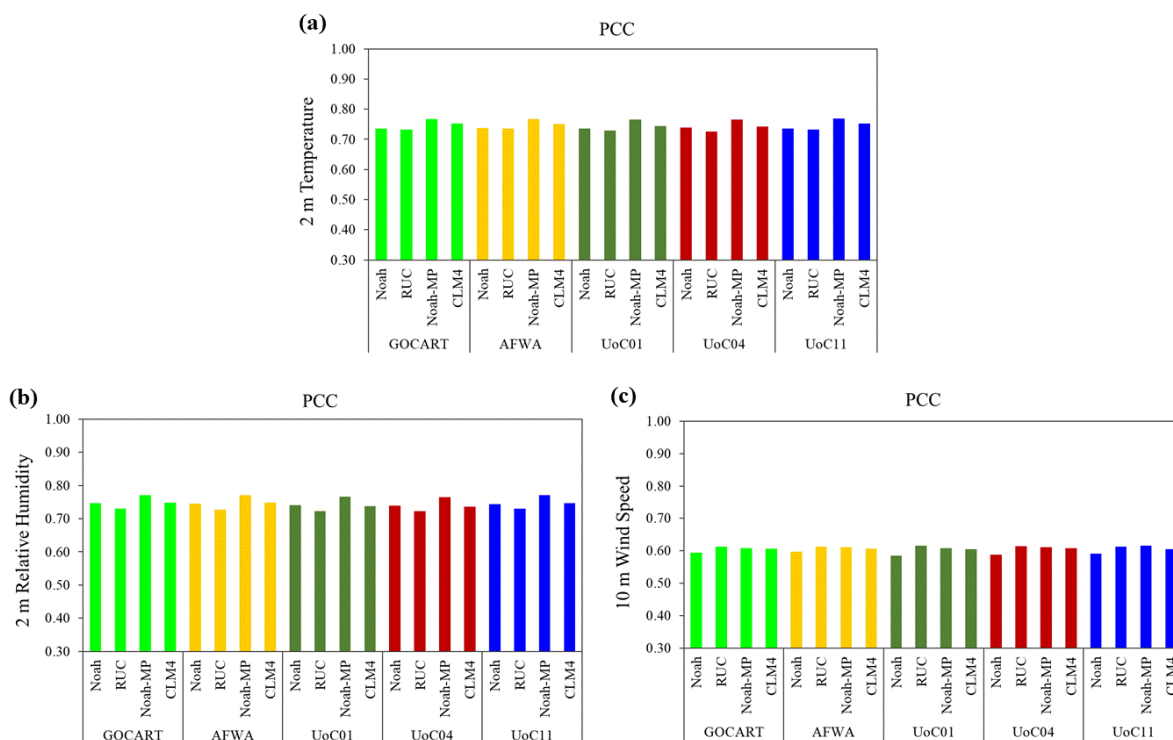


Figure 4: Pearson's correlation coefficient (PCC) of all scheme combinations for (a) T2m, (b) RH2m, and (c) WS10m, respectively, using the ASOS data. The y-axis represents values greater than 0.3, indicating the minimum threshold for a weak correlation. The values are averaged over the stations (see Fig. 3c).

(Revised manuscript) Figure 6

→ We adjusted the positions of the blue in (a) and modified the caption accordingly.

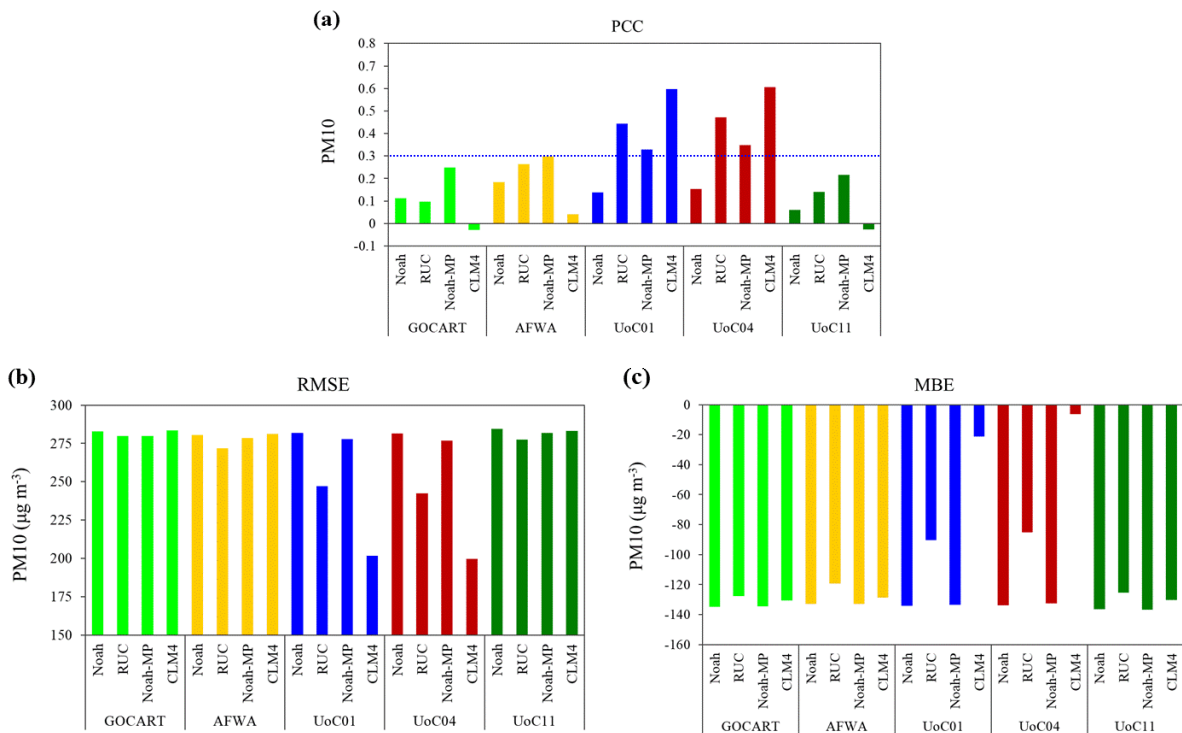


Figure 6: The verification results of all experiments for PM10 concentrations; (a) PCC, (b) RMSE, and (c) MBE, respectively, using the in-situ data. Based on PCC values, the blue dashed line represents the minimum threshold for a moderate correlation. The values are averaged over the stations (see Fig. 3c).

(Revised manuscript) Lines 360 ~ 361

In all scheme combinations except for combinations of UoC04 and UoC01 with CLM4 and RUC, PCC was below 0.3, indicating a weak or almost no correlation; ~

5. By my understanding, no forecasts were produced in this study (i.e., there was no attempt to predict the future). So, “forecasted” values is really referring to “modeled” or “simulated” values. (Line 346, 351, and elsewhere)

→ We appreciate the reviewer’s comment. We agree with the reviewer's comments and believe that the term “modeled” or “simulated” is more appropriate than “forecasted” in this study. So, we have revised all the relevant content as follows.

(Revised manuscript) Figure 5

→ We have changed 'Forecast' on the y-axis in Figure 5 to 'Simulation' and 'forecasted' in the caption to 'simulated'.

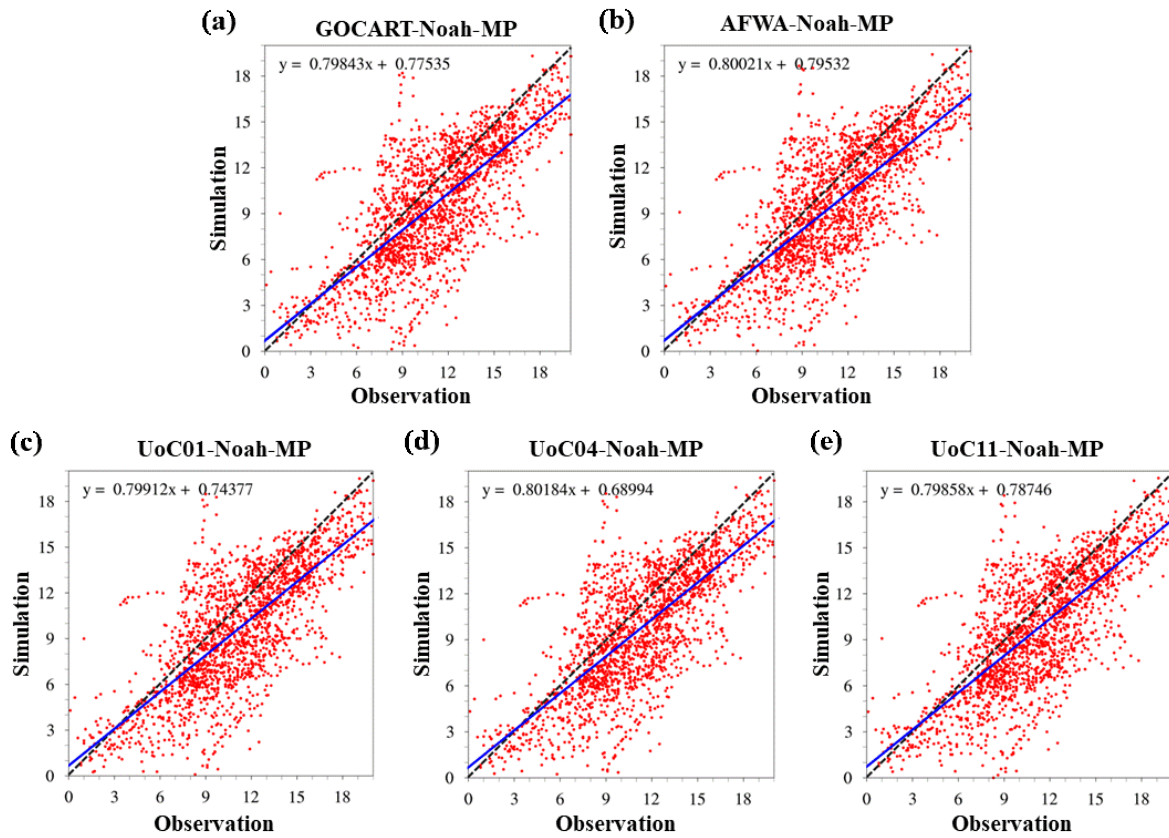


Figure 5: Scatter plots showing the relationship between observed and simulated values for T2m, using Noah-MP-based combinations. Each panel represents a different scheme combinations: (a) GOCART-Noah-MP, (b) AFWA-Noah-MP, (c) UoC01-Noah-MP, (d) UoC04-Noah-MP, and (e) UoC11-Noah-MP. The black dashed line represents that the simulation perfectly matches the observation. The blue line indicates the linear regression fit to the data, providing relationship between the observed and simulated values.

→ We have also changed 'Forecast' on the y-axis in Figure 7 and Figure S3 to 'Simulation'.

Reply to the Comments by Reviewer #2 on GMD-2024-114

“ Evaluation of Dust Emission and Land Surface Schemes in Predicting a Mega Asian Dust Storm over South Korea Using WRF-Chem (v4.3.3)”

By Ji Won Yoon, Seungyeon Lee, Ebony Lee, and Seon Ki Park

Formal Review

This paper describes the performance of the WRF-Chem model in simulating a strong Asian dust event with combinations of different dust emissions and land surface schemes. The selection of dust emission and land surface schemes in simulating dust events is sometimes quite challenging as studies have shown discrepancies in simulating dust events with different dust emission and land surface schemes. So, understanding how the combination of dust emission and land surface schemes can simulate dust events is important to improve dust event forecasting skills and to reduce immediate downwind impact on many effects, including air quality, human health, road safety, etc. So, I find the goal of the paper interesting, and it can contribute knowledge in identifying and possible improvement of dust event simulation with WRF-Chem. It can add value to regional dust event forecasting.

However, the paper is more focused on data comparison and did not explain the underlying causes for why different combinations of land surface and dust emission schemes simulated dust events differently. Also, meteorological forcing is one of the important aspects of dust event formation, however, the paper did not explain the meteorological phenomena for different combinations of schemes. I have pointed out a few major concerns and specific comments separately, below.

Both major concerns and specific comments need to be addressed to increase the quality of the manuscript. So, I recommend this paper for major revision.

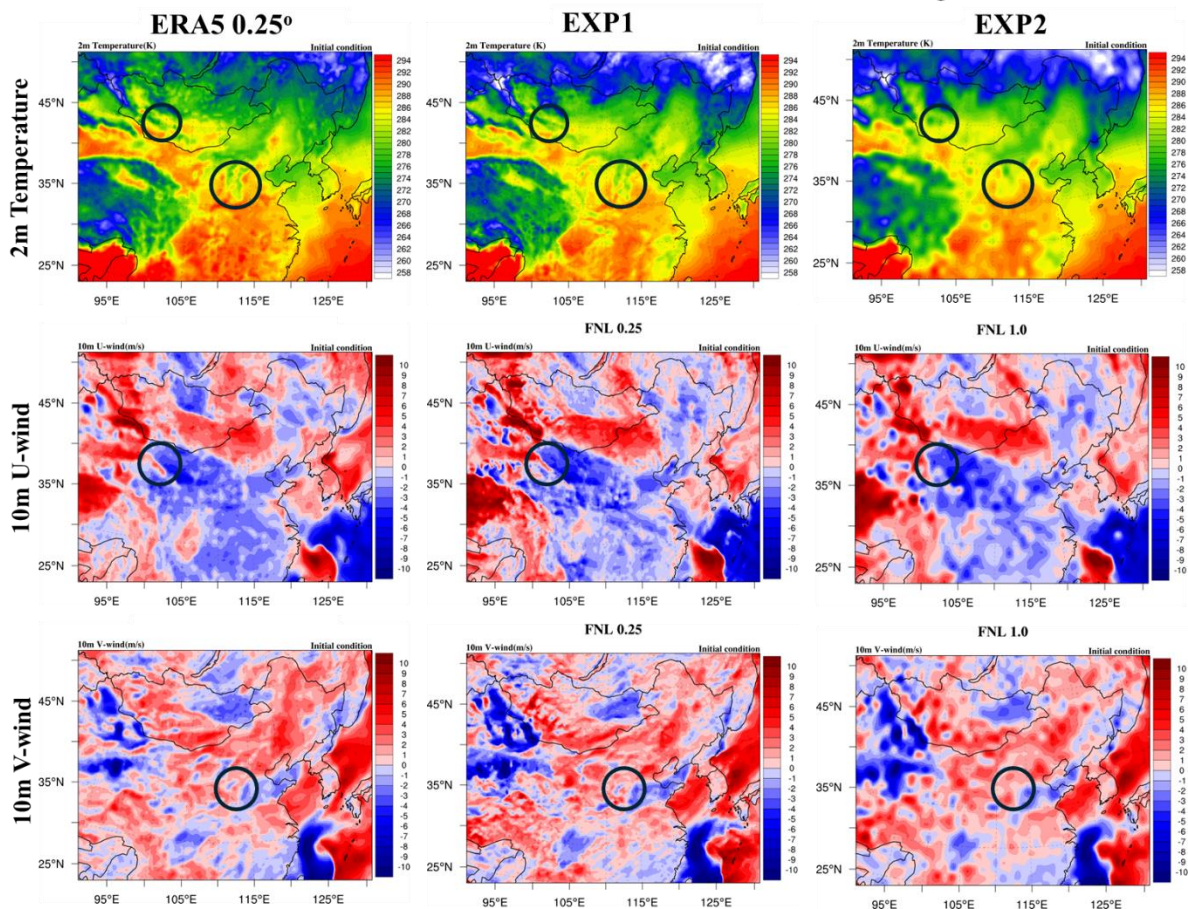
→ We sincerely appreciate your thoughtful review and valuable comments, which have greatly helped us improve our manuscript. We have carefully addressed each of your comments and provided a detailed, point-by-point response below.

Major Comments

1. Why the simulation domain grid resolution is coarser (30 km) than the initial and boundary conditions forcing data FNL 0.25 degrees? Why do authors upscale instead of downscaling the simulation?

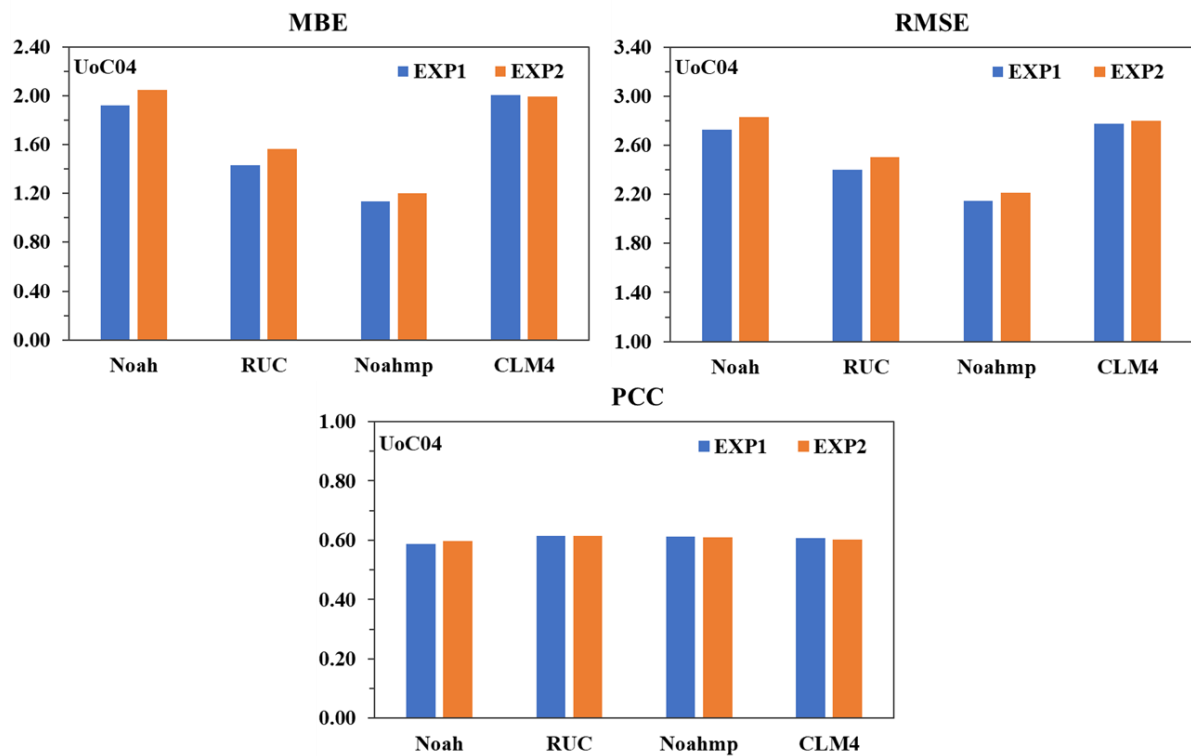
→ We appreciate the reviewer for pointing this out. The FNL 0.25° (~25 km) dataset provides a finer resolution than the FNL 1.0° (~100 km) dataset. Given the model resolution of 30 km in this study, we decided to upscale the FNL 0.25° dataset to generate initial and boundary conditions. This approach minimizes information loss and retains more detailed spatial information compared to downscaling the FNL 1.0° dataset. Furthermore, it is expected to reduce boundary discontinuities. Below, we present a comparison of initial conditions generated using the FNL 0.25° and FNL 1.0° datasets, with ERA5 0.25° as a reference, in terms of 2 m temperature, 10 m U-wind, and 10 m V-wind. EXP1 demonstrates a more detailed spatial distribution than EXP2 and better reflects the finer structures similar to those in ERA5.

- **EXP1:** Initial conditions at 30 km resolution using **FNL 0.25° data**
- **EXP2:** Initial conditions at 30 km resolution using **FNL 1.0° data**



Additionally, to address part of the comment regarding “Lines 316-317”, which the reviewer mentioned in a similar context, we conducted additional sensitivity experiments (EXP2: combinations of all land surface schemes and UoC04). The 10 m wind speed was evaluated using MBE, RMSE, and PCC metrics. This evaluation utilized data from 26 ASOS stations in South Korea, consistent with the previous validation method. The following are the validation results: 1) For MBE, UoC04-CLM4 shows very similar values between EXP1 (2.0) and EXP2 (1.99), whereas all other scheme combinations indicate that EXP1 exhibits smaller MBE values compared to EXP2; 2) For RMSE, EXP1 consistently showed smaller values than EXP2 for UoC04-based combinations; 3) For PCC, both EXP1 and EXP2 show similar values across UoC04-based combinations, indicating that the two experiments exhibit comparable linear correlation with the observed data.

- **EXP1:** Upscaled to 30 km resolution from FNL 0.25° data
- **EXP2:** Downscaled to 30 km resolution from FNL 1.0° data°



2. Though the focus of the study is sensitivity analysis, the explanation of underlying causes that resulted in discrepancies in dust event simulation is important to explain. In general, we all know different land surface models perform differently, but having a large set of simulation results, the paper would benefit from some explanation on why and how different land surface models simulated dust events differently. I suggest adding some discussion to the result section to explain why different combinations resulted in different simulation results.

→ We appreciate your insightful comment. As the reviewer pointed out, discussing how different combinations led to differences in the simulations will significantly enhance the quality and clarity of the manuscript. To address this, we have added ‘subsection 3.3’ to provide a more detailed discussion and clarify the impacts of different scheme combinations.

(Revised manuscript)

3.3 Impact of scheme combinations on dust emission

The sensitivity experiments showed that each scheme combination produced different simulation results for meteorological variables and air quality variables over South Korea, with notable differences in PM₁₀, AOD, and DUST. To identify the underlying causes of these differences, we analysed the meteorological conditions and surface DUST at the source regions for each scheme combination. The analysis focused on a specific point (44.18°N, 110.61°E) (see Fig. 3a) in the source regions where high MODIS AOD was observed during the dust emission period (see Fig. 12a). In general, in dust source regions, higher 2m temperature, lower 2m relative humidity, and stronger 10m wind speed increase the probability of dust occurrence—high temperature and low humidity dry the surface, making it easier for dust particles to be lifted, and strong winds transport the dust into the atmosphere (Yang et al., 2019). Figure S12 shows the time series of DUST, T_{2m}, RH_{2m}, and WS_{10m} for UoC04-based combinations at the analysis point. The light orange shading indicates the period with the higher T_{2m}, lower RH_{2m}, stronger WS_{10m}, and the initial increase in DUST. Overall, the meteorological variables varied depending on the scheme combination but were consistent with the general conditions required for dust emission. Notably, higher DUST concentrations were observed in UoC04-CLM4 and UoC01-CLM4, whereas lower concentrations were found in UoC04-Noah and UoC04-Noah-MP (Fig. S12a). These differences reflect the unique characteristics of each land surface scheme, despite using the same UoC04 parameterization.

In general, aeolian erosion, which contributes to dust emission in arid and semi-arid regions, occurs when the friction velocity is greater than the threshold value. Threshold values vary depending on soil properties and conditions, such as soil texture, particle size, and soil moisture (Fécan et al., 1999). The

UoC schemes first calculate u_{*t} for dry and bare surface and then incorporate surface roughness features and soil moisture content to derive a more realistic threshold friction velocity (Shao and Lu, 2000). The calculation of u_{*t} is as follows:

$$u_{*t} = u_{*t}(dry_{bare})f_r f_s, \quad (13)$$

where $u_{*t}(dry_{bare})$ represents the threshold friction velocity for dry and bare surfaces; f_r indicates roughness features, and f_s denotes soil moisture content (Fécan et al., 1999). f_r is calculated based on the drag partition theory, whereas f_s is explicitly related to the land surface model. The latter is computed using the following equation:

$$f_s = \sqrt{1 + a(i)(S - S_{dry}(i))^{b(i)}}, \quad (14)$$

where i represents the soil texture index, which ranges from 1 to 12 (e.g., 1: sand, 2: loamy sand, 3: sandy loam, etc.); $a(i)$, $b(i)$ and $S_{dry}(i)$ indicate tabulated parameter values corresponding to the soil texture index, respectively. Here, S represents soil moisture, and $S_{dry}(i)$ denotes the dry soil moisture threshold at which direct evaporation from the topsoil layer ends. This threshold varies depending on the land surface schemes, influencing the explicit calculation of different u_{*t} values and ultimately playing a significant role in the dust emission process.

Figure 15 shows the time series of DUST, u_{*t} and u_* for UoC04-based combinations. The light orange shading marks periods of simulated dust emission. The DUST concentrations showed significant differences depending on the land surface scheme. Details are as follows: 1) In the first shaded period, UoC04-CLM4 exhibited the highest DUST concentration, followed by UoC04-RUC, UoC04-Noah-MP, and UoC04-Noah. In the second, the DUST concentrations were lower than in the first, with UoC04-RUC exhibiting the highest concentration, followed by UoC04-CLM4. In contrast, UoC04-Noah-MP and UoC04-Noah showed DUST concentrations close to zero (Fig. 15a); 2) For UoC04-Noah, u_* barely exceeded u_{*t} in the first period, resulting in very low DUST concentrations, whereas in the second period, u_* did not exceed u_{*t} , leading to DUST concentrations close to zero (Fig. 15b); 3) For UoC04-RUC, u_* significantly exceeded u_{*t} in both the first and second shaded periods, resulting in high DUST concentrations (Fig. 15c); 4) For UoC04-Noah-MP, u_* exceeded u_{*t} in the first period, but only slightly exceeded it during the second period, resulting in very low dust concentrations in the first period and nearly zero in the second (Fig. 15d); 5) For UoC04-CLM4, a pattern similar to UoC04-RUC was observed, with u_* greatly exceeding u_{*t} , leading to high DUST concentrations (Fig. 15e). In conclusion, UoC04-RUC and UoC04-CLM4 exhibited higher DUST concentrations despite u_* being similar to or even smaller than that of UoC04-Noah-MP. This results from the relatively lower u_{*t} in UoC04-RUC and UoC04-CLM4 compared to UoC04-Noah-MP, allowing u_* to exceed the

threshold more easily. Additionally, the greater difference between u_{*t} and u_* contributed to the observed higher DUST concentrations. This highlights the interaction between dust emission schemes and land surface schemes, emphasizing the complexity of physical processes and surface-atmosphere interactions.

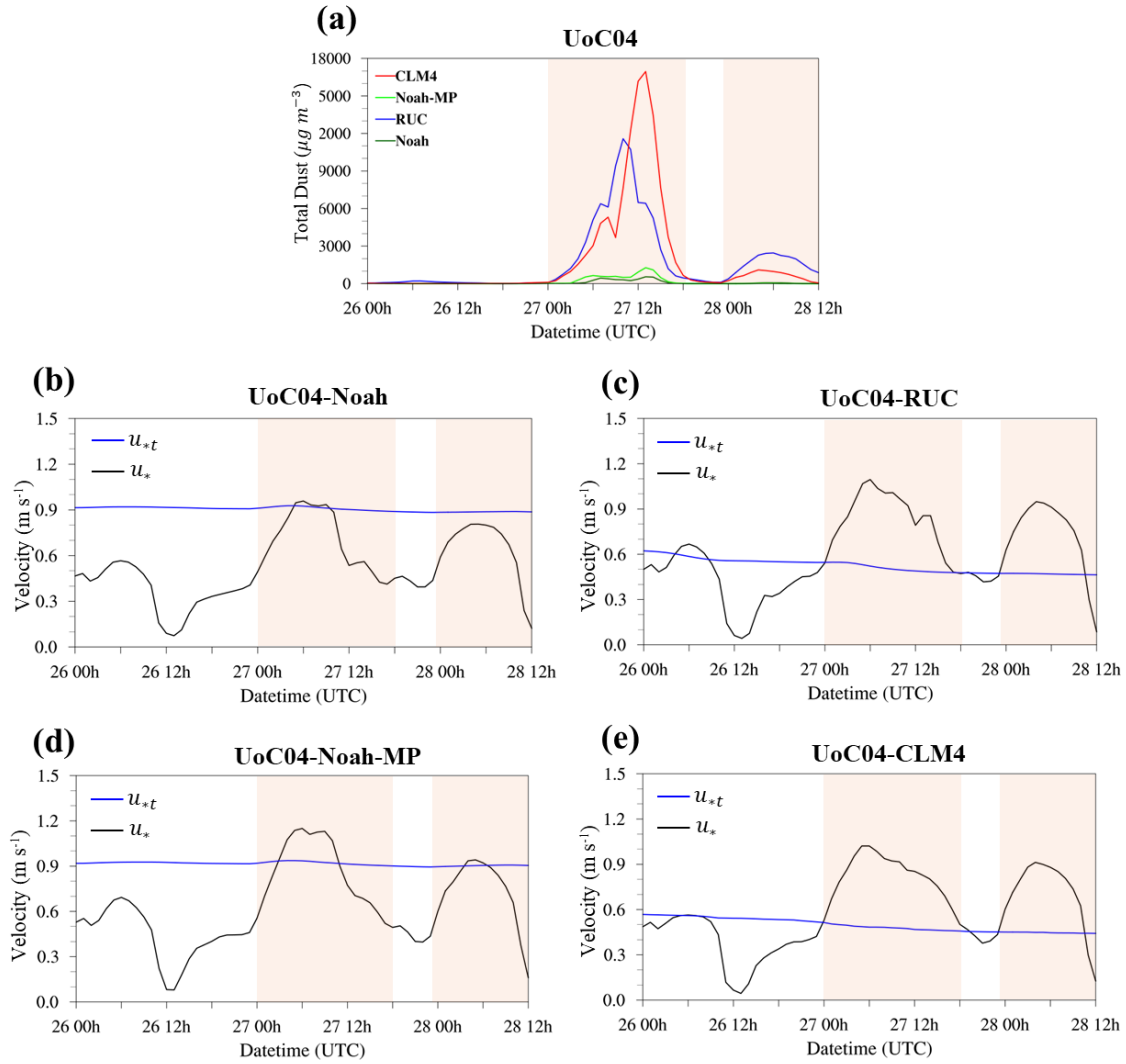


Figure 15: Hourly time series of surface DUST, threshold friction velocity (u_{*t}), and friction velocity (u_*) for combinations of all land surface schemes and UoC04. The light orange shadings indicate the periods of simulated dust emission: (a) surface DUST concentrations, u_{*t} , and u_* for (b) UoC04-Noah, (c) UoC04-RUC, (d) UoC04-Noah-MP, and (e) UoC04-CLM4.

Figure S13 shows the time series of DUST, T2m, RH2m, and WS10m for CLM4-based combinations at the analysis point. The UoC04-CLM4 showed the highest DUST concentrations, followed by UoC01-CLM4, while the other combinations exhibited significantly lower values. For T2m, RH2m, and WS10m, CLM4-based combinations showed similar patterns until their maximum or minimum values were reached. Afterward, UoC04-CLM4 and UoC01-CLM4, which simulated the highest DUST concentrations, exhibited distinct patterns compared to the other combinations—dust blocks or absorbs solar radiation, affecting temperature and humidity, thereby altering atmospheric thermal stability, which can influence the wind (Darvishi Boloorani et al., 2021). These differences reflect the unique characteristics of each dust emission scheme, despite using the same land surface model CLM4.

The GOCART-based schemes (GOCART and AFWA) and the UoC-based schemes (UoC01, UoC04, and UoC11) differ significantly in calculating dust emission flux. The GOCART-based schemes directly incorporate the dust erodibility factor into the calculation of dust emission flux, whereas the UoC-based schemes primarily use it as a dust source indicator. Additionally, the GOCART-based schemes use the porosity, whereas the UoC schemes account for various vegetation and soil physical properties—soil bulk density, vegetation fraction, disturbed particle size distribution, and soil plastic pressure—to enhance the accuracy of simulations (Zhao et al., 2020). Each scheme can be examined in detail as follows: 1) GOCART tends to overestimate u_t , leading to underpredictions of dust emissions, particularly for smaller particles (LeGrand et al., 2019); 2) AFWA, a modified version of GOCART, improves accuracy by replacing u_t with u_{*t} . It also incorporates soil clay content and aerodynamic roughness length, enabling more precise dust emission simulations; 3) UoC01 provides a more realistic representation of soil particle types by incorporating the size distribution of airborne dust particles, constrained by minimally disturbed $p_m(d_i)$ and fully disturbed $p_f(d_i)$ states (see Eq. 5). Naturally, dust particles generally exist as coatings on sand grains in sandy soils or as aggregates in clay-rich soils. In weak wind erosion, dust-coated sand particles and clay aggregates act as individual units and may not be released, representing a minimally disturbed state. In contrast, strong winds break them apart, increasing dust emissions in a fully disturbed state; 4) The UoC04 is simplified compared to UoC01 but still considers $p_m(d_i)$ and $p_f(d_i)$; 5) The UoC11 does not account for $p_m(d_i)$ and $p_f(d_i)$, thereby removing the kinematic impact on dust particle size distribution (Shao et al., 2011; see Eq. 8). This improves computational efficiency but reduces the accuracy of dust emission simulations. Consequently, as shown in Fig. S13a, the simulated DUST concentrations are low.

These differences in dust emission schemes led to distinct dust simulation results, even when the same land surface scheme was applied. In the CLM4-based combinations, UoC04 and UoC01 simulated high DUST concentrations in the source region (Fig. S13a), which were then transported to South Korea (Fig. 8). In contrast, GOCART, AFWA, and UoC11 failed to simulate both dust emissions and transport

(Fig. S13a and Fig. 8). These findings are similar to those of Lee et al. (2022), which emphasized the sensitivity of dust emission schemes to dust events in South Korea.

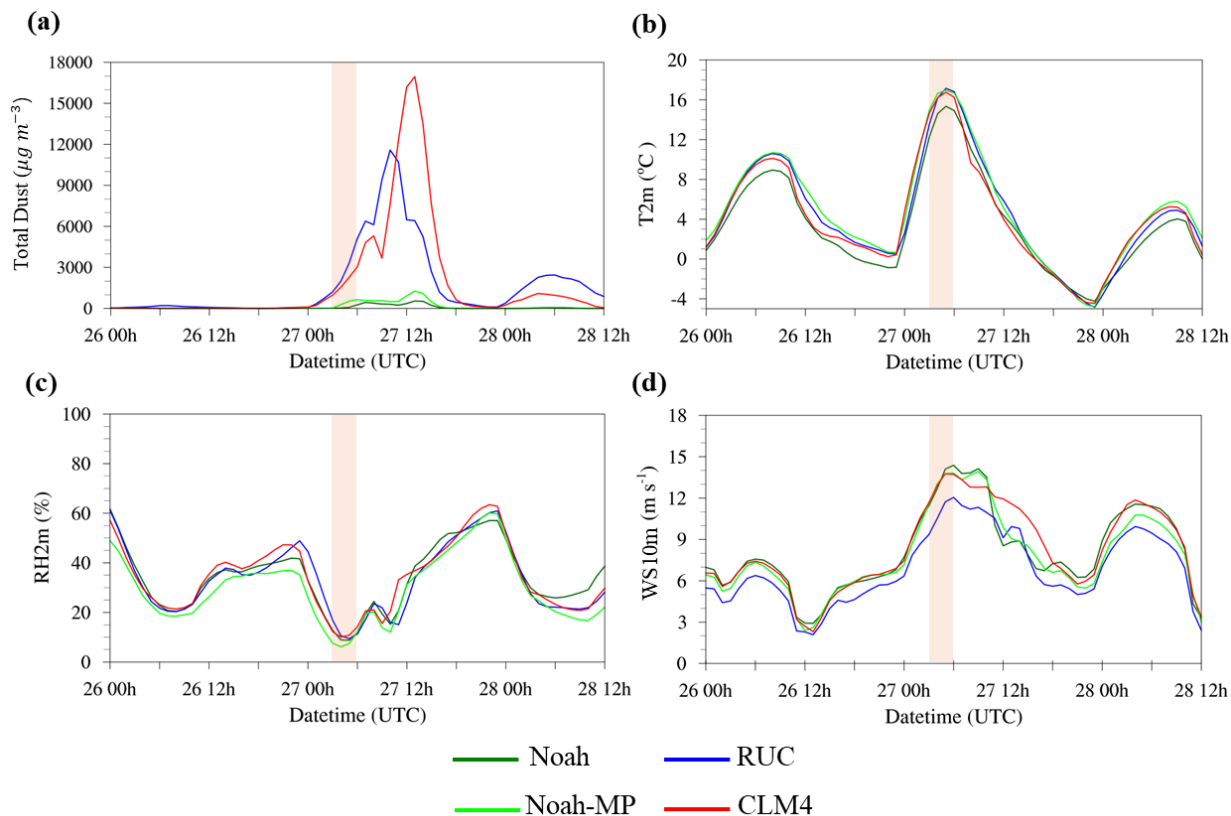


Figure S12: Time series comparison of (a) DUST, (b) T2m, (c) RH2m, and (d) WS10m. The colored lines depict various scheme combinations, and the light orange shadings indicate the period with initial DUST increase: the green for UoC04-Noah, the blue for UoC04-RUC, the lime green for UoC04-Noah-MP, and the red for UoC04-CLM4.

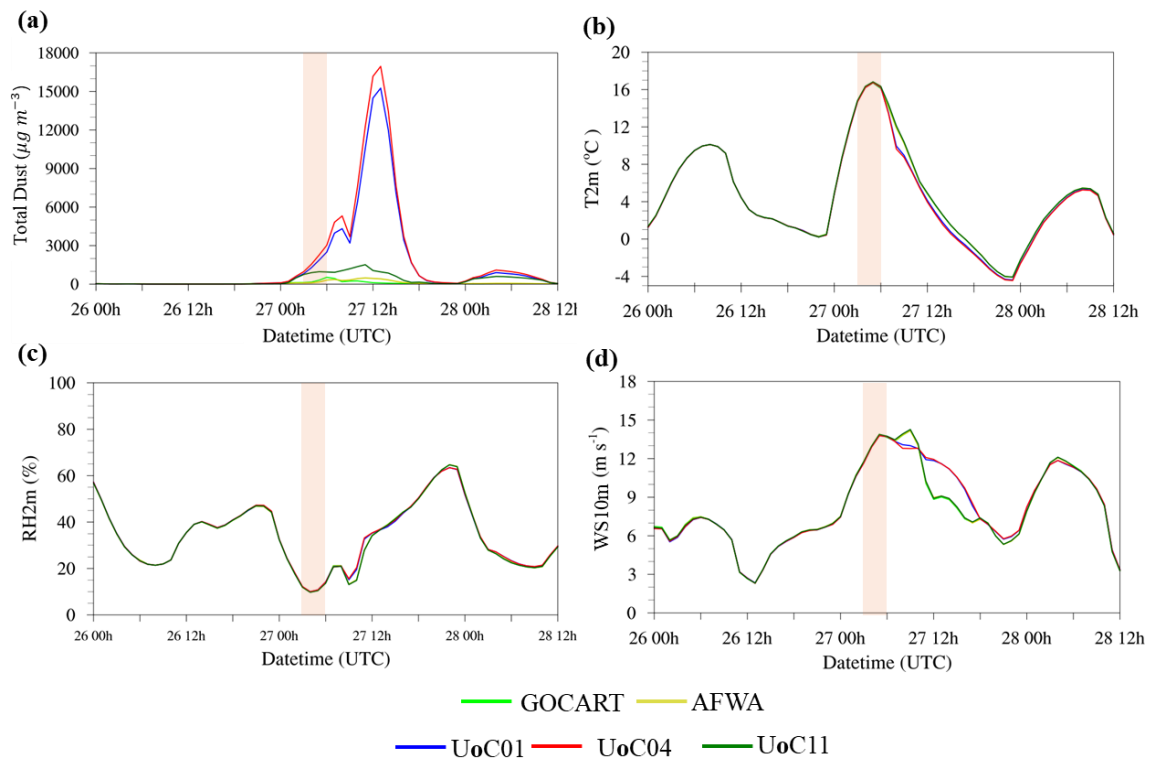


Figure S13: Same as in Fig. S12 but for combinations of all dust emission schemes and CLM4: the lime green for GOCART-CLM4, the yellow for AFWA-CLM4, the blue for UoC01-CLM4, the red for UoC04-CLM4, and the green for UoC11-CLM4.

3. Meteorological forcing is very important for dust event formation. Having a comparison between simulated and reanalysis near-surface wind allows us to evaluate how the model simulated near-surface wind, which is critical for dust emission and transport. Yes, the paper presented correlation analysis for 10m wind to compare observational data across South Korea (downwind sink region) but the near-surface wind condition upwind (across the source region) is completely unknown. We need to evaluate how the model performed near the source area as well to have more confidence on our simulation results that our simulation also reasonably reproduced near-surface wind at the source. Authors can add spatial evolution of near-surface wind (e.g., 10m wind) from FNL/MERRA-2 and compare with WRF-Chem simulation.

→ We sincerely appreciate your thoughtful review. As the reviewer pointed out, near-surface wind in the source region is a critical factor for dust emission and transport, and its evaluation is essential. Based on the MODIS AOD results (see Fig.12a), we identified areas with high AOD in the source region at the time of the dust emission, including a specific part of the Gobi Desert (see Fig. 3a). For this area, we validated the 10 m wind speed from all experiments against MERRA-2 data, using MBE, RMSE and PCC. Additionally, we compared the spatial and temporal evolution of dust, along with the 10m wind, between the simulation results and MERRA-2 data to evaluate how well the model represented the role of wind in contributing to dust emission and transport processes. For reference, MERRA-2 provides total dust concentrations at 3-hour intervals. We have added the following content to the manuscript.

(Original manuscript)

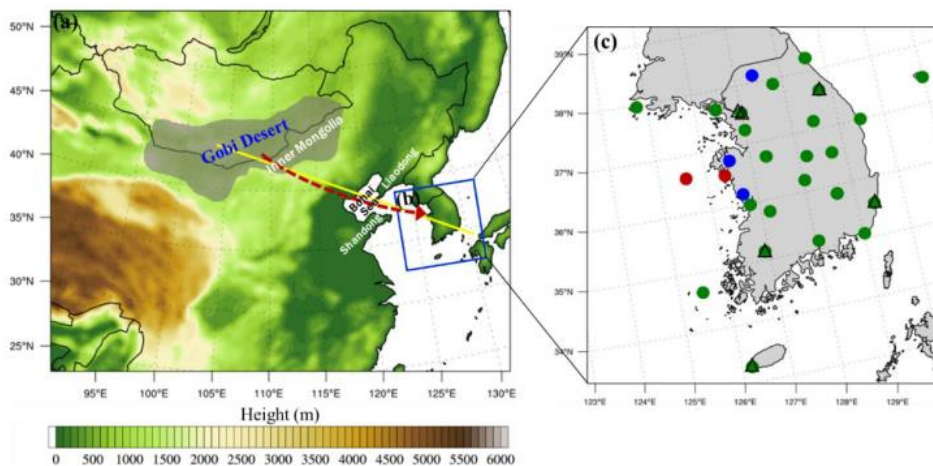


Figure 3: The computational domain with WRF-Chem for (a) simulation, (b) verification against in-situ and AERONET data in South Korea, and (c) locations of the ASOS, Asian dust observation stations, and AERONET used for verification: In (a), the gray shadings represent the ADSs source regions for this study case, and the red dashed arrow indicates the main route of ADSs. The solid yellow line denotes the location for vertical cross-section analysis

(see Fig. 11 and Fig. S7). In (c), the green circles indicate the locations where the ASOS and Asian dust observation stations coexist---23 stations; the blue circles represent ASOS stations only---3 stations; the red circles depict Asian dust observation stations only---2 stations; and the black triangle indicates AERONET sites---6 sites.

(Revised manuscript) #1

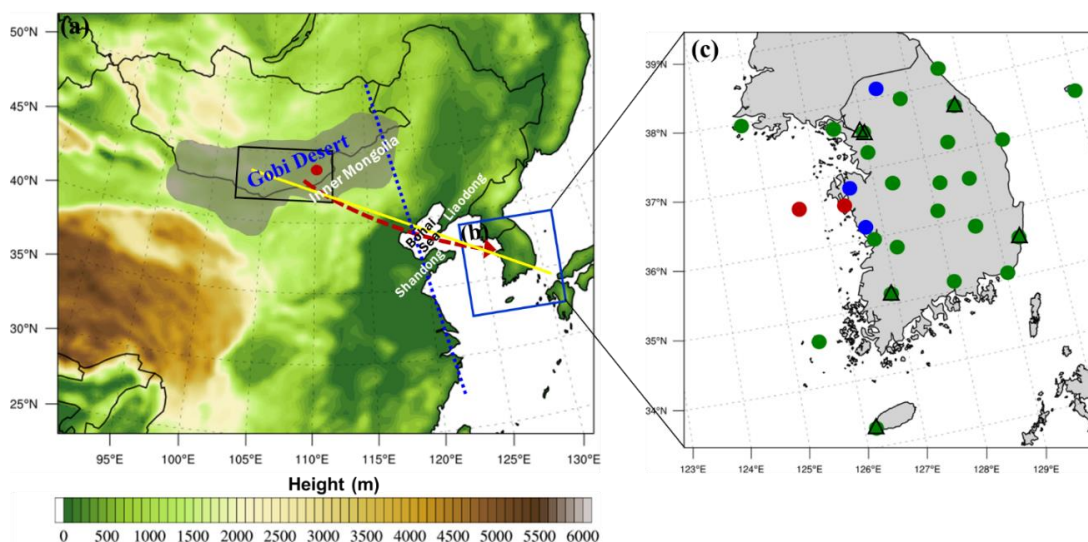


Figure 3: The computational domain with WRF-Chem for (a) simulation, (b) verification against in-situ and AERONET data in South Korea, and (c) locations of the ASOS, Asian dust observation stations, and AERONET used for verification: In (a), the gray shading represents the ADSs source regions for this study case, and the red dashed arrow indicates the main route of ADSs. The yellow solid line denotes the location for vertical cross-section analysis (see Figs. 14 and S11), and the blue dotted line represents the CALIPSO orbit path (see Figs. 13 and S10). In the ADSs source regions, the black square box denotes the area used for verification (see Fig. 10), and the red circle indicates the specific location for additional analysis (see Subsection 3.3). In (c), the green circles indicate the locations where the ASOS and Asian dust observation stations coexist—23 stations; the blue circles represent ASOS stations only—3 stations; the red circles depict Asian dust observation stations only—2 stations; and the black triangles indicate AERONET sites—6 sites.

3.2.2 Surface wind speed: MERRA-2

The near-surface wind across the source region is a critical factor for dust emission and transport. We identified areas with high values in the source region based on the MODIS AOD (see Fig. 12a) and validated WS10m from all experiments in this region against MERRA-2 data using MBE, RMSE, and PCC metrics. Figure 10 shows PCC, RMSE, and MBE for all scheme combinations. Consistent with the previous verification results for meteorological variables over South Korea, the scheme combinations with the same land surface scheme showed similar performance. The detailed verification results are as follows: 1) For PCC, all experiments exhibited high values ranging from 0.83 to 0.89. The PCC values of the scheme combinations using CLM4- and RUC-based combinations were relatively higher than those using Noah- and Noah-MP-based combinations (Fig. 10a); 2) For RMSE, UoC04-CLM4 (1.81) and UoC01-CLM4 (1.81) exhibited the same lowest values (Fig. 10b). These scheme

combinations showed the best performance in PM10 verification over South Korea; 3) For MBE, the scheme combinations based on Noah-MP showed positive MBE values, whereas the others exhibited negative MBE values. The CLM4-based combinations had the smallest magnitude of negative MBE of around -0.02 (Fig. 10c). Overall, the CLM4-based combinations, including UoC04-CLM4 and UoC01-CLM4—which demonstrated good performance in predicting PM10 and AOD over South Korea—also showed the best performance for WS10m in the source region.

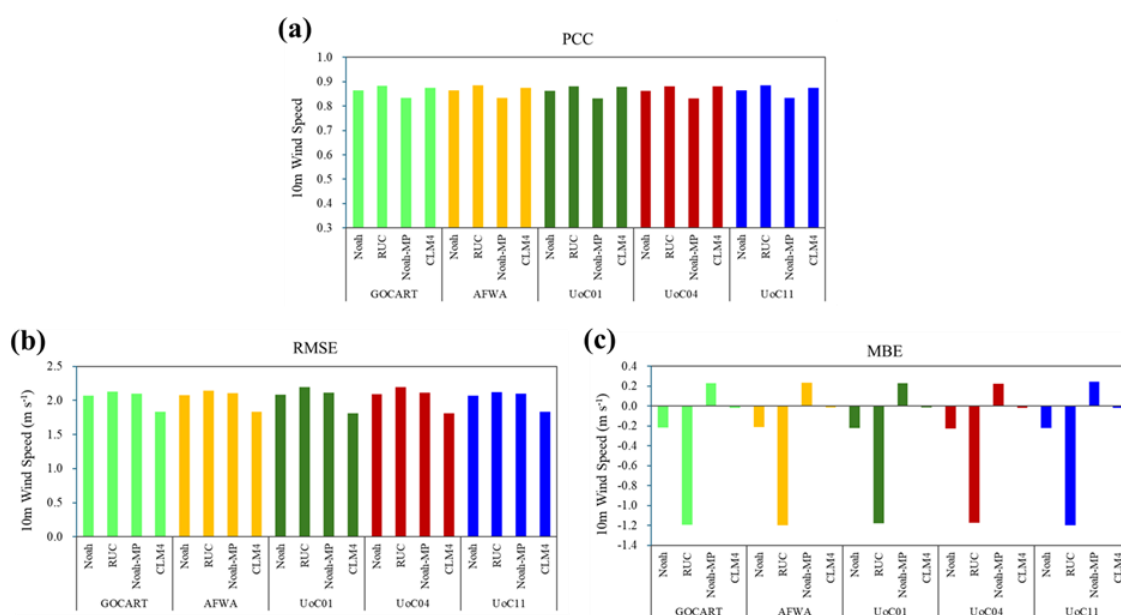


Figure 10: Verification results of all experiments for 10 m wind speed in the source region; (a) PCC, (b) RMSE, and (c) MBE, respectively, using the MERRA-2. The values are averaged over grid points of MERRA-2 (see Fig. 3a).

(Revised manuscript) #2

Figure 11 shows the spatial evolution of surface total dust (DUST) concentrations and 10 m wind for CLM4-based combinations. Both MERRA-2 and the CLM4-based combinations similarly formed strong north-westerly winds in the source region, creating favourable conditions for dust emission and transport. However, MERRA-2, GOCART-CLM4, AFWA-CLM4, and UoC11-CLM4 exhibited significantly lower dust concentrations, whereas UoC04-CLM4 and UoC01-CLM4 showed notably higher concentrations (Fig. 11a). Subsequently, despite similar wind between MERRA-2 and CLM4-based combinations, only UoC04-CLM4 and UoC01-CLM4 successfully transported dust toward the Bohai Sea with strong north-westerly winds (Fig. 11b). As a result, UoC04-CLM4 and UoC01-CLM4 successfully transported dust to South Korea, reproducing a high-concentration dust event (Fig. 11c).

These results are evident in comparison to MODIS AOD observations (see Fig. 12), as MERRA-2, GOCART-CLM4, AFWA-CLM4, and UoC11-CLM4 significantly underestimated dust concentrations, whereas UoC04-CLM4 and UoC01-CLM4 provided more reliable results.

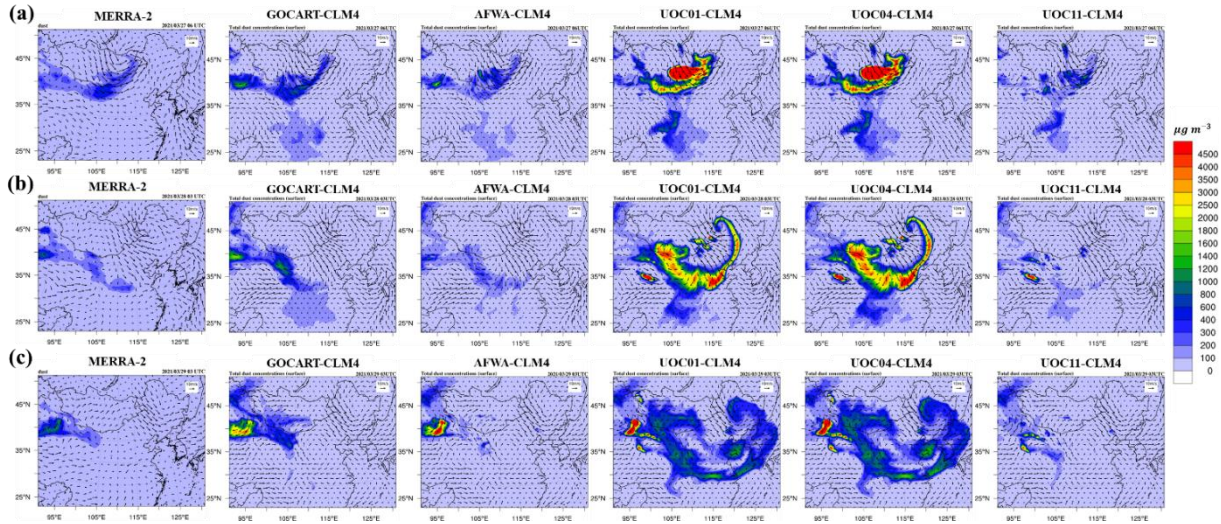


Figure 11: Spatial distribution of surface DUST concentrations ($\mu\text{g m}^{-3}$) and 10m wind (m s^{-1}) in the model domain for MERRA-2, and combinations of all dust emission schemes and CLM4: (a) dust emission in the Gobi/Inner Mongolia desert at 0600 UTC on March 27, (b) transport towards the Bohai Sea at 0300 UTC on March 28, (c) appearance in South Korea at 0300 UTC on March 29, 2021.

Figure S8 is the same as Figure 11, except for the UoC04-based combinations. The wind patterns in the dust emission and transport processes were similar between MERRA-2 and the UoC04-based combinations in the source region (Fig. S8a and b). However, as dust was transported into South Korea, the wind over the West Sea was weaker in MERRA-2 but stronger in the UoC04-based combinations (Fig. S8c). In terms of dust concentrations, UoC04-RUC and UoC04-CLM4 provided the most reliable simulations overall.

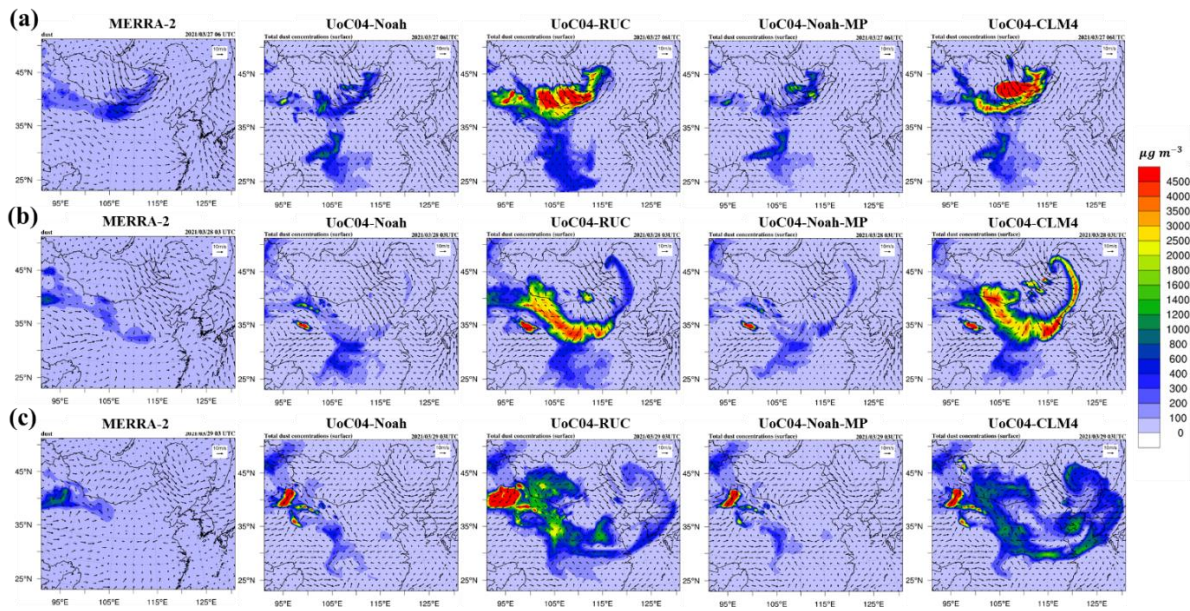


Figure S8: Same as in Fig. 11 but for combinations of all land surface schemes and UoC04.

Specific and minor comments

Lines 3-4: “Using WRF-Chem (v4.3.3)”

I suggest removing WRF-Chem version in the title.

→ We appreciate the reviewer’s comment. We have removed the WRF-Chem version from the title.

(Original manuscript)

Evaluation of Dust Emission and Land Surface Schemes in Predicting a Mega Asian Dust Storm over South Korea Using WRF-Chem (v4.3.3)

(Revised manuscript)

Evaluation of Dust Emission and Land Surface Schemes in Predicting a Mega Asian Dust Storm over South Korea Using WRF-Chem

Lines 28-29: “exerting significant impacts on human life and health”

Please provide some references here.

→ We appreciate the reviewer for pointing this out. We have added relevant references.

(Revised manuscript)

exerting significant impacts on human life and health (Zhang et al., 2016)

Zhang, X., Zhao, L., Tong, D.Q., Wu, G., Dan, M., Teng, B.: A systematic review of global desert dust and associated human health effects. *Atmos.* 7(12), 158. <https://doi.org/10.3390/atmos7120158>, 2016.

Line 35: “spring season”

Provide months

→ We appreciate the reviewer’s comment. We have added months to clarify the spring season.

(Revised manuscript)

spring season (March to May)

Line 39: “literally meaning”

“Literally meaning” or “Literal meaning”?

→ We appreciate the reviewer for pointing this out. We have revised it to "literal meaning."

(Original manuscript)

The SDSs are also named Hwangsa in Korean, literally meaning ‘yellow sands’.

(Revised manuscript)

The SDSs are also named Hwangsa in Korean, which has the literal meaning of ‘yellow sands’.

Lines 42-44: “The Weather Research and Forecasting (WRF) model coupled with Chemistry (WRF-Chem; Grell et al., 2005) has been extensively employed for simulating and forecasting the weather and air quality (i.e., trace gases, aerosols, etc.) variables.”

Provide some references here.

→ We appreciate the reviewer for pointing this out. We have added relevant references.

(Revised manuscript)

The Weather Research and Forecasting (WRF) model coupled with Chemistry (WRF-Chem; Grell et al., 2005) has been extensively employed for simulating and forecasting the weather and air quality (i.e., trace gases, aerosols, etc.) variables (Chen et al., 2014; Kumar et al., 2014; Liu et al., 2016; Thomas et al., 2019; Wang et al., 2021).

Chen, S., Zhao, C., Qian, Y., Leung, L. R., Huang, J., Huang, Z., Bi, J., Zhang, W., Shi, J., Yang, L., Li, D., and Li, J.: Regional modeling of dust mass balance and radiative forcing over East Asia using WRF-Chem, *Aeolian Res.*, <https://doi.org/10.1016/j.aeolia.2014.02.001>, 2014.

Kumar, R., Barth, M. C., Pfister, G. G., Naja, M., and Brasseur, G. P.: WRF-Chem simulations of a typical pre-monsoon dust storm in northern India: Influences on aerosol optical properties and radiation budget, *Atmos. Chem. Phys.*, <https://doi.org/10.5194/acp-14-2431-2014>, 2014.

Liu, L., Huang, X., Ding, A., and Fu, C.: Dust-induced radiative feedbacks in north China: A dust storm episode modeling study using WRF-Chem, *Atmos. Environ.*, <https://doi.org/10.1016/j.atmosenv.2016.01.019>, 2016.

Thomas, A., Huff, A. K., Hu, X. M., and Zhang, F.: Quantifying uncertainties of ground-level ozone within WRF-Chem simulations in the mid-Atlantic region of the United States as a response

to variability, *J. Adv. Model. Earth Syst.*, **11**, 1100–1116, <https://doi.org/10.1029/2018MS001457>, 2019.

Wang, W., Luo, C., Sheng, L., Zhao, C., Zhou, Y., and Chen, Y.: Effects of biomass burning on chlorophyll-a concentration and particulate organic carbon in the subarctic North Pacific Ocean based on satellite observations and WRF-Chem model simulations: a case study, *Atmos. Res.*, **254**, 105526, <https://doi.org/10.1016/j.atmosres.2021.105526>, 2021.

Lines 51-52: “In WRF-Chem, the dust emission flux mainly depends on the soil type and the near-surface winds (Kok et al., 2012; Shao, 2008) within the dust emission scheme”

Since we are discussing how dust emission flux is calculated inside the WRF-Chem, better reference would be the papers that describes dust emission flux calculation inside the WRF-Chem. For example, Legrand et al. (2019) <https://doi.org/10.5194/gmd-12-131-2019>.

Also, is soil type more important than surface roughness in dust emission? Look at the dust emission flux calculation equation in dust emission schemes. I suggest looking at a few latest research that describes how important surface roughness is for dust emission processes.

→ We sincerely appreciate your thoughtful review. Following your comments, we have revised the references on dust emission flux calculation and added references on the importance of surface roughness in the dust emission process.

(Original manuscript)

In WRF-Chem, the dust emission flux mainly depends on the soil type and the near-surface winds (Kok et al., 2012; Shao, 2008) within the dust emission scheme. Conversely, soil moisture, vegetation, and snow can influence changes in dust emission flux (Ginoux et al., 2001; Park et al., 2010),

(Revised manuscript)

In WRF-Chem, the dust emission flux depends on various factors, including soil type, near-surface winds, soil moisture, surface roughness, vegetation, snow, and others within the dust emission scheme (Ginoux et al., 2001; Laurent et al., 2013; Legrand et al., 2019; Park et al., 2010; Rubinstein et al., 2020; Singh et al., 2017),

Rubinstein, D., et al.: Dust emission thresholds in loess soil under different saltation fluxes, *Appl. Sci.*, **10**, 5949, <https://doi.org/10.3390/app10175949>, 2020.

Singh, C., Ganguly, D., and Dash, S. K.: Dust load and rainfall characteristics and their relationship

over the South Asian monsoon region under various warming scenarios, *J. Geophys. Res.- Atmos.*, 122, <https://doi.org/10.1002/2017JD027451>, 2017.

Line 52: “Conversely, soil moisture, vegetation, and snow can influence changes in dust”

Should not be “conversely”. You are describing other contributing variables that impact dust emission flux.

→ We appreciate the reviewer for pointing this out. We kindly request that you refer to the comment for ‘Lines 51-52’ for further details.

Lines 83-86: “by using in-situ, including the Automated Surface Observing System (ASOS) and Asian dust observation data, remote sensing data, including the AErosol RObotic NETwork (AERONET) and the MODerate resolution Imaging Spectroradiometer(MODIS), and reanalysis data such as Modern-Era Retrospective Analysis for Research and Applications, version 2 (MERRA2)”

You can include all these in the data and method section.

→ We appreciate the reviewer’s suggestion. Following the reviewer’s comment, we have included this content in the ‘Data and Method section’.

(Original manuscript)

by using in-situ, including the Automated Surface Observing System (ASOS) and Asian dust observation data, remote sensing data, including the AErosol RObotic NETwork (AERONET) and the MODerate resolution Imaging Spectroradiometer 85 (MODIS), and reanalysis data such as Modern-Era Retrospective Analysis for Research and Applications, version 2 (MERRA2), over South Korea.

(Revised manuscript)

The sentence was removed and relocated to Section 2.4, "Evaluation Data and Methods."

2.4 Evaluation data and methods

We evaluated the performance of scheme combinations using three types of data: in-situ data, including the Automated Surface Observing System (ASOS) and Asian dust observation data; remote sensing data, including the AErosol RObotic NETwork (AERONET), Cloud-Aerosol Lidar and Infrared Pathfinder Satellite Observation (CALIPSO), and the MODerate resolution Imaging Spectroradiometer (MODIS); and reanalysis data, including Modern-Era Retrospective Analysis for Research and

Applications, version 2 (MERRA-2).

Lines 105-106: “Fig. 1”

See your figure caption. I suggest not to abbreviate if not abbreviated in caption. Please be consistent throughout the text.

→ We appreciate the reviewer for pointing this out. We have revised the manuscript following the GMD author guidelines. Specifically, we ensured that no abbreviations are used at the beginning of sentences throughout the manuscript.

Lines 135-136: “a grid spacing of 30 km and 50 vertical levels up to 50 hPa.”

Is there any reason for making grid resolution coarser (30km) than meteorological initial and boundary condition data (0.25 degrees)?

→ We appreciate the reviewer’s detailed comment. We have provided a response to ‘Major Comment 1’ related to this comment. We kindly request that you refer to it for more information.

Lines 137-141: “The meteorological initial and boundary conditions are obtained from the global final analysis (FNL) dataset with a resolution of $0.25^\circ \times 0.25^\circ$, produced by the Global Forecast System (GFS) of the National Centers for Environmental Prediction (NCEP); the boundary conditions are updated every 6 h. The chemical initial and boundary conditions are derived from the Community Atmosphere Model with Chemistry (CAM-chem), part of the National Center for Atmospheric Research (NCAR)’s Community Earth System Model (CESM) and are produced using the mozbc pre-processing tool”

Better to provide links or references for used data sources.

→ We appreciate the reviewer for pointing this out. We have added links to the data sources used.

(Revised manuscript)

The meteorological initial and boundary conditions are obtained from the global final analysis (FNL; <https://rda.ucar.edu/datasets/ds083.3/dataaccess>) dataset with a resolution of $0.25^\circ \times 0.25^\circ$, produced by the Global Forecast System (GFS) of the National Centers for Environmental Prediction (NCEP); the boundary conditions are updated every 6 h. The chemical initial and boundary conditions are derived from the Community Atmosphere Model with Chemistry (CAM-chem; <https://www.acom.ucar.edu/cam-chem/cam-chem.shtml>), part of the National Center for Atmospheric

Research (NCAR)'s Community Earth System Model (CESM) and are produced using the mozbc pre-processing tool (<https://www.acom.ucar.edu/wrf-chem/download.shtml>).

Lines 316-317: “The scheme combinations generally have good performance with high to moderate PCCs for surface meteorological variables: 0.73–0.77 for T2m, 0.73–0.77 for RH2m, 0.58–0.62 for WS10m”

Here we can see the PCC for WS10m ranged between 0.58-0.62. Wind speed being the primary control of dust emission, accurate simulation of windspeed is important. From the correlation analysis, we can see how observed and modeled data are related but we will not have sufficient information on model performance. For example, whether the model output was overestimated or underestimated throughout the dust event period at a particular station. This is critically important if we are assessing the model's performance to investigate when the model is not able to work well. So, my suggestion is to add a time series plot as PM10 timeseries plot for different meteorological variables for different stations. This will enable us to find where and when the model is doing better performance.

→ We appreciate the reviewer for pointing this out. The PM10 observation sites mostly overlap with the ASOS observation sites, so we selected two of the six PM10 time series sites for representation. This decision was based on the observation that the time series data for meteorological variables showed similar characteristics across the sites.

(Revised manuscript)

Figure S3 shows time series comparisons of observations and CLM4-based combinations of T2m (Fig. S3a), RH2m (Fig. S3b), and WS10m (Fig. S3c), at two ASOS stations in South Korea—Yeongwol and Cheonan. The time series of T2m, RH2m, and WS10m showed very similar patterns, as meteorological variables are generally influenced more by land surface schemes than by dust emission schemes. For T2m, CLM4-based combinations showed an underestimation trend, whereas RH2m and WS10m tended to be overestimated. In particular, RH2m reached nearly 100% before the ADS entered South Korea due to precipitation from a passing low-pressure system. The north-westerly winds behind this system, driven by an accompanying high-pressure system, often transport ADS from Inner Mongolia and the Gobi Desert to South Korea in spring (Lee et al., 2016). Meanwhile, despite the similar time series patterns of T2m, RH2m, and WS10m in the CLM4-based combinations, the PM10 time series showed that GOCART-CLM4, AFWA-CLM4, and UoC11-CLM4 failed to reproduce the observed values (see Fig. 8). This failure is attributed to the inability to simulate dust emissions at the source regions, resulting in the absence of ADS transport to South Korea (see Figs. 12 and S9).

Figure S4 is the same as Figure S3, except for UoC04-based combinations. T2m, RH2m, and WS10m showed significant differences based on the land surface schemes. Similar to the CLM4-based combinations, T2m was underestimated, whereas RH2m and WS10m were overestimated. For T2m, UoC04-Noah-MP closely matched the observations during the daytime, whereas UoC04-RUC performed better at night. For RH2m, UoC04-RUC, UoC04-Noah-MP, and UoC04-CLM4 matched the observations during periods of decreasing relative humidity, although UoC04-RUC showed noticeable differences. However, during periods of increasing RH2m, UoC04-based combinations differed significantly from the observations. For WS10m, UoC04-Noah and UoC04-CLM4 showed greater overestimation compared to UoC04-RUC and UoC04-Noah-MP.

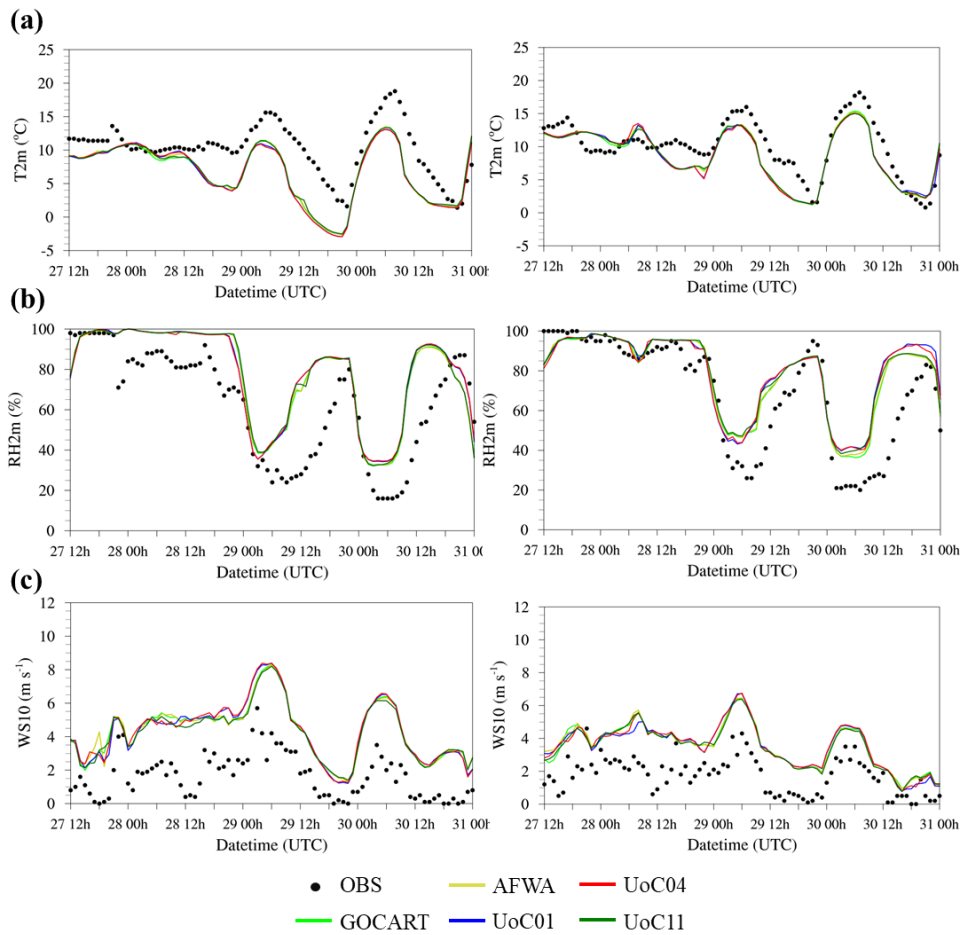


Figure S3. Time series comparison of T2m, RH2m, and WS10m between observations and combinations of all dust emission schemes and CLM4. The left panels represent Yeongwol, and the right panels Cheonan, with (a) T2m, (b) RH2m, and (c) WS10m. The black dots represent the observations, whereas the colored lines depict various scheme combinations: the lime green for GOCART-CLM4, the yellow for AFWA-CLM4, the blue for UoC01-CLM4, the red for UoC04-CLM4, and the green for UoC11-CLM4.

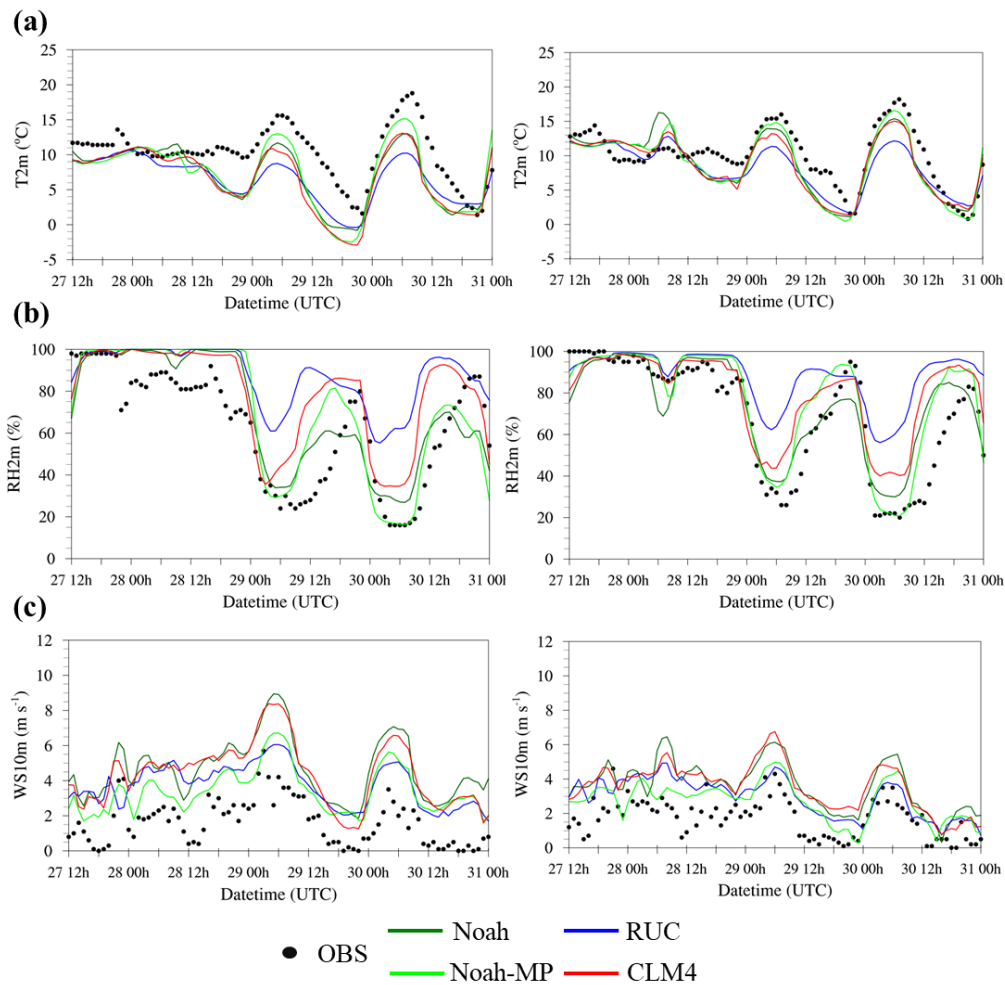


Figure S4: Same as in Fig. S3 but for the combinations of all land surface schemes and UoC04: the green for UoC04-Noah, the blue for UoC04-RUC, the lime green for UoC04-Noah-MP, and the red for UoC04-CLM4.

Topography can influence wind speed simulation, especially in complex terrain. The simulated wind at 30km is very coarse. As I pointed out earlier, the simulation grid resolution is coarser than its boundary conditions data, which might have introduced some discrepancies between observed and simulated values.

Since, in most cases, CPP values for 30km resolution are similar. I would add another sensitivity case for at least one case to check what if we downscale wind speed and how it affects CPP.

→ We appreciate the reviewer’s detailed comment. We have addressed this in our response to “Major Comment 1”. We would be grateful if you could refer to this.

Lines 327-330: “Fig. S2 shows the MBE for all scheme combinations: 1) For T2m, Noah-MP- and Noah-based combinations showed similarly large MBEs, with a negative trend across all experiments (Fig. S2a); 2) For RH2m, Noah-MP- and Noah-based combinations also showed similarly good performance, with positive bias across all experiments (Fig. S2b); 3) For WS10m, 330 Noah-MP-based combination showed the best performance, with positive bias (Fig. S2c).”

An average MBE provides over/under-estimation of a given value, however, does not provide enough information on which geographic location (station) simulated results closely match with observed data. This hinders how the model performs at different geographic locations during the dust event. I would suggest making a time series plot at different locations. This will enable how the model performs at different geographic locations and help to investigate what are the possible reasons behind observed and simulated discrepancies.

→ We appreciate the reviewer’s suggestion. We have addressed this in our response to “Lines 316-317”, and we kindly request you to refer to it for further details.

Line 421: “and Mungyeong: UoC04-CLM4 and UoC01-CLM showed”

Possible typo. “UoC01-CLM” should be “UoC01-CLM4”.

→ We appreciate the reviewer’s suggestion. We have corrected the typo.

Line 457: “depicting the processes of dust origination”

Depiction of AOD does not explain the dust origination. It provides spatial evolution of the dust, but not the dust origination. Please correct language throughout this section.

→ We appreciate the reviewer for this valuable comment. We have thoroughly reviewed the use of the term 'origination' throughout the manuscript and revised the relevant parts as follows.

Lines 23-24:

However, both UoC04-CLM4 and UoC01-CLM4 simulated values closest to the MODIS AOD but tended to overestimate the AOD in some regions during the origination and transportation processes.

→ However, both UoC04-CLM4 and UoC01-CLM4 simulated values closest to the MODIS AOD but tended to overestimate the AOD in some regions during the dust emission and transportation processes.

Line 457: Figure 10 shows the spatial distribution of AOD depicting the processes of dust origination

(Fig. 10a), transportation (Fig. 10b), and appearance in South Korea (Fig. 10c) in comparison of MODIS (i.e., observation) with MERRA-2 (i.e., reanalysis) and combinations of dust emission schemes and CLM4 (i.e., model results).

→ Figure 12 shows the spatial distribution of AOD, comparing dust evolution processes—dust emission (Fig. 12a), transport (Fig. 12b), and appearance in South Korea (Fig. 12c)—among MODIS (i.e., observation), MERRA-2 (i.e., reanalysis), and combinations of dust emission schemes and CLM4 (i.e., model results).

Line 460:

At 0500 UTC on March 27, 2021 (Fig. 10a), dust origination stage, ~

→ At 0500 UTC on March 27, 2021 (Fig. 10a), dust emission stage, ~

Line 465:

due to the absence of dust origination in the source region ~

→ due to the absence of dust emission in the source region

Line 482:

(a) dust origination in the Gobi/Inner Mongolia desert at 0500 UTC on March 27, ~

→ (a) dust emission in the Gobi/Inner Mongolia desert at 0500 UTC on March 27, ~

Line 547:

Finally, we found that UoC01-CLM4 and UoC04-CLM4 effectively simulated the three processes of origination, transport, and appearance in South Korea, ~

→ Finally, we found that UoC04-CLM4 and UoC01-CLM4 effectively simulated the three processes of emission in source region, transport, and appearance in South Korea, ~

Line 470: “In summary, while UoC01-CLM4 and UoC04-CLM4 effectively simulated the processes of dust origin”

Similar to previous comment. Not dust origin but spatial evolution of the dust.

→ We appreciate the reviewer’s valuable comment. Following the reviewer’s suggestion, we have replaced 'processes of dust origin' with 'spatial evolution of the dust' to more accurately reflect the manuscript.

(Original manuscript)

In summary, while UoC01-CLM4 and UoC04-CLM4 effectively simulated the processes of dust origin, transportation, and appearance in South Korea

(Revised manuscript)

In summary, while UoC04-CLM4 and UoC01-CLM4 effectively simulated the spatial evolution processes of dust in South Korea

Lines 486: “3.2.3 Vertical distributions of dust concentrations”

This section presents the time evolution of vertical distribution of dust from different simulations and lacks comparison with observations. Without comparing it with observational datasets, it is hard to investigate which simulation reproduced the vertical evolution of the dust.

If there is any data source (e.g., CALIPO product) that can be used to compare vertical evolution of the dust. I suggest exploring this option or there might be other way.

→ We appreciate the reviewer’s suggestion. Figures 11 and S7 show only the differences in the vertical evolution of total dust concentrations across various scheme combinations; The purpose of these figures was to examine the differences in the vertical evolution of total dust concentrations across the various combinations. We fully agree with the reviewer that comparing these results to observations is essential for improving the quality of this manuscript. CALIPSO, a satellite-based lidar, provides observations of the vertical distribution of aerosols, but its coverage is limited to specific observation times and orbital paths. Therefore, we compared the aerosol extinction coefficients from CALIPSO with the experimental results, considering the satellite’s orbit paths and observation times.

(Revised manuscript) #1

2.4.2 Remote sensing data

The CALIPSO carries an aerosol lidar that measures the vertical structure of the atmosphere using an Orthogonal Polarimeter. It provides aerosol extinction coefficients at 532 nm and 1064 nm, as well as column AOD data in the troposphere and stratosphere (Vaughan et al., 2004; Winker et al., 2003). In this study, vertical profiles of aerosol extinction coefficients at 532 nm (CAL_LID_L2_05kmAPro-Standard-V4-21; Vaughan et al., 2004) were used to evaluate the vertical structure of modeled dust concentrations

3.2.4 Vertical distributions of extinction coefficients and dust concentrations: CALIPSO

Figure 13 shows a comparison of the vertical profiles of extinction coefficients between simulations (550 nm)—using CLM4-based combinations—and CALIPSO observations (532 nm). At 0500 UTC on March 28, the CALIPSO orbit passed through the Bohai Bay, including the Shandong Peninsula (see Fig 3a), where high extinction coefficients were observed (117–120°E and 36–41°N) (Fig. 13a). Compared to the CALIPSO observations, overall, the extinction coefficients in the UoC04-CLM4 and UoC01-CLM4 are consistent with the observations, particularly in regions with high values over the Bohai Bay and the Shandong Peninsula (Figs. 13d and e). In contrast, GOCART-CLM4, AFWA-CLM4, and UoC11-CLM4 significantly underestimate the values. This finding is consistent with the MODIS AOD (see Fig. 12b) and supports the reliability of the vertical distributions of DUST concentrations from the scheme combinations (see Fig. 14b).

Figure S10 is the same as Figure 13, except for the UoC04-based combinations. UoC04-CLM4 showed the greatest similarity to the observations (Fig. S10e), whereas UoC04-RUC simulated a too-narrow horizontal extent of high extinction coefficients (Fig. S10c). In contrast, UoC04-Noah and UoC04-Noah-MP significantly underestimate the values (Figs. S10b and d).

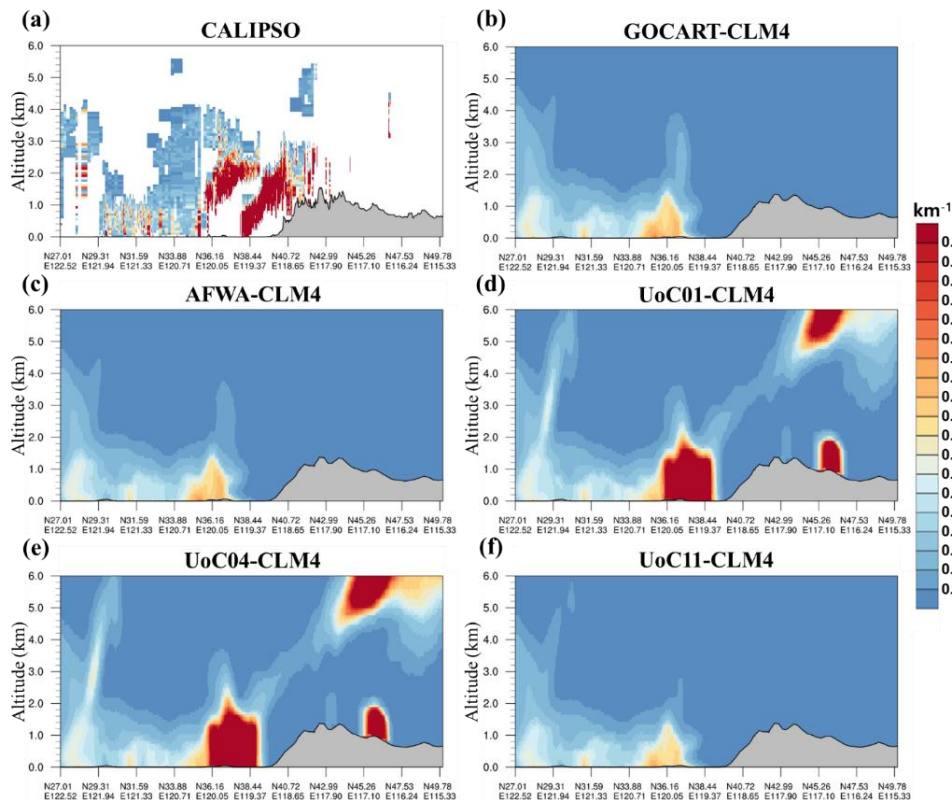


Figure 13: Vertical distributions of aerosol extinction coefficient for (a) CALIPSO, (b) GOCART-CLM4, (c) AFWA-CLM4, (d) UoC01-CLM4, (e) UoC04-CLM4, and (f) UoC11-CLM4 at 0500 UTC on March 28, 2021. Blue dotted lines in Fig. 3a represent the sectional paths.

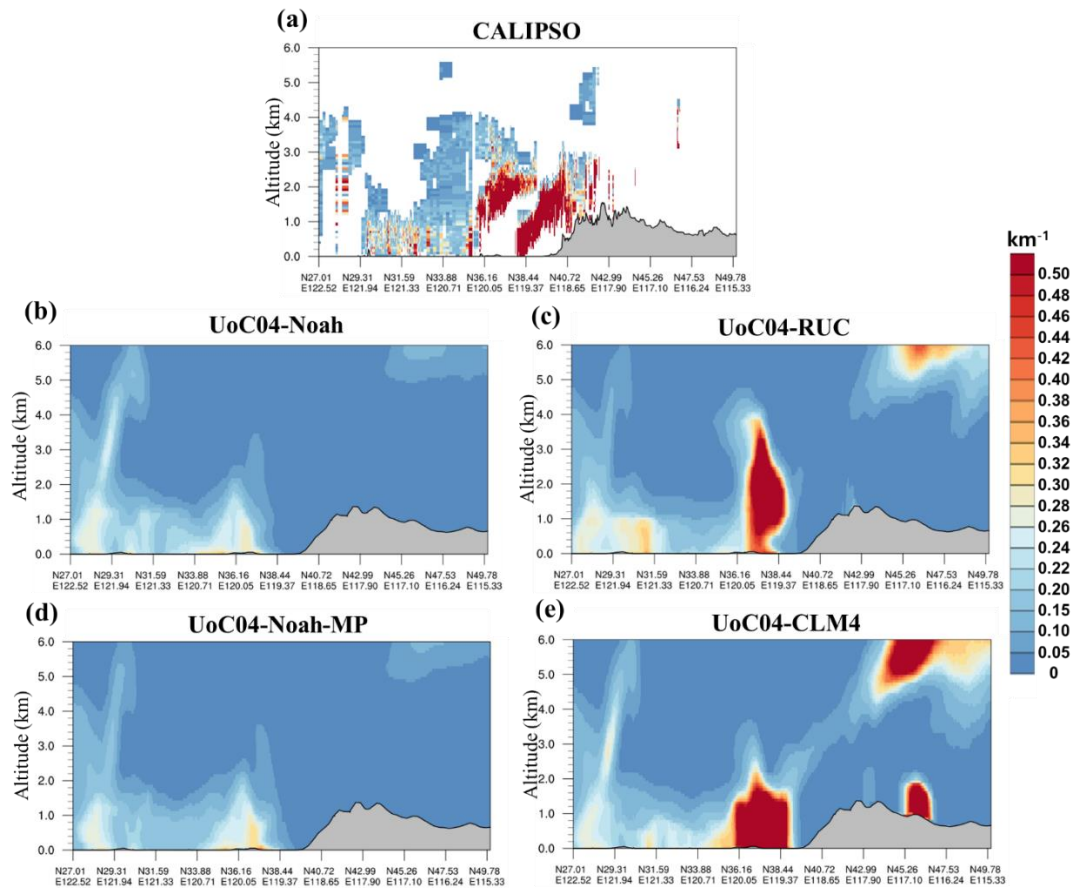


Figure S10: Same as in Fig. 13 but for the combinations of all land surface schemes and UoC04—(a) CALIPSO, (b) UoC04-Noah, (c) UoC04-RUC, (d) UoC04-Noah-MP, (e) UoC04-CLM4.

Line 523: “This study aims to evaluate the performance various combinations of parameterization schemes”

Language is not clear, please make it clearer.

→ We appreciate the reviewer for pointing this out. We have revised the sentence for clarity.

(Original manuscript)

This study aims to evaluate the performance various combinations of parameterization schemes ~

(Revised manuscript)

This study aims to evaluate the performance of various combinations of parameterization schemes ~

Lines 532-534: “They were verified against surface observation data using various static metrics: 1) It turns out that the land surface schemes have a greater effect on surface meteorological variables than the dust emission schemes—showing little difference in model performance using different dust emission schemes”

Our general understanding is that different land surface schemes perform differently. Readers might want to know the possible reasons why different land surface schemes along with different dust emissions schemes performed differently. Most of the results presented here just show how different models are performing differently, but the underlying reasons why different land surface models perform differently are absent. This is particularly important to address why some schemes are doing a good job while others are not. Please see my major comments section for more details.

→ We appreciate the reviewer’s valuable comment. We have addressed this in our response to ‘Major Comment 2’. We would be grateful if you could refer to this.

Lines 534-539: “Additionally, the combinations of all dust emission and Noah-MP schemes, known for its excellence as a land surface scheme, showed the best performance; 2) For surface PM10 concentrations, we observed significant variations of prediction performance across different scheme combinations, as the dust emission schemes directly influence the generation of dust storms. UoC04-CLM4 showed the best performance, followed by UoC01-CLM4, UoC04-RUC, and UoC01-RUC. In contrast, other scheme combinations showed very poor performance and failed to predict PM10 in this study.”

This is a very interesting result. Dust emission with Noah-MP schemes showed the best performance for dust emission while for PM10, UoC04-CLM4 showed the best performance. The PM10 concentration comes from transported dust. So, dust emission and transport mechanism (meteorology behind dust transport) might have played a different role. Is there a forcing mechanism (dust emission and subsequent transport) is more important than land surface schemes? This needs to be investigated to separate the effect of schemes and forcing mechanisms. Authors have not described the underlying differences between different land surface schemes inhibiting why different schemes resulted in different results. Please see my major comments also.

→ We appreciate the reviewer’s insightful comment. The manuscript's explanation may not have been

entirely clear, potentially leading to some misunderstanding. The sentence “Additionally, the combinations of all dust emission and Noah-MP schemes, known for its excellence as a land surface scheme, showed the best performance” corresponds to “1) It turns out that the land surface schemes have a greater effect on surface meteorological variables than the dust emission schemes—showing little difference in model performance using different dust emission schemes. Additionally, the combinations of all dust emission and Noah-MP schemes, known for its excellence as a land surface scheme, showed the best performance”.

In other words, this sentences do not indicate that Noah-MP schemes performed best for dust emission but rather highlights their good performance in surface meteorological variables. Therefore, we have revised the sentence as follows.

(Original manuscript)

Additionally, the combinations of all dust emission and Noah-MP schemes, known for its excellence as a land surface scheme, showed the best performance.

(Revised manuscript)

Notably, the combinations of all dust emission and Noah-MP schemes, known for its excellence as a land surface scheme, showed the best performance for meteorological variables.

Also, we have addressed this in our response to ‘Major Comment 2’. We kindly request you to refer to it for further details.

Further revisions by the author

Additionally, we made the following revisions based on the reviewer's comments. We fully agree with the reviewer's emphasis on the importance of near-surface wind. While the reviewer did not specifically mention Fig. 5, we replaced the scatter plot of 2 m temperature in Fig. 5 for South Korea (downwind sink region) with a scatter plot of 10 m wind. The revised Fig. 5 now presents the 10 m wind scatter plot for UoC04-based combinations. This change was made based on validation results indicating that meteorological variables are more influenced by land surface schemes than by dust emission schemes.

(Original manuscript)

Figure 5 shows the scatter diagram for T2m of Noah-MP-based combinations, which exhibited the best performance for T2m, RH2m, and WS10m in the verification. Consistent with the verification results,

the dust emission scheme does not significantly impact the linear correlation between observed and simulated surface meteorological variables. Similar outcomes were observed for RH2m and WS10m (not shown).

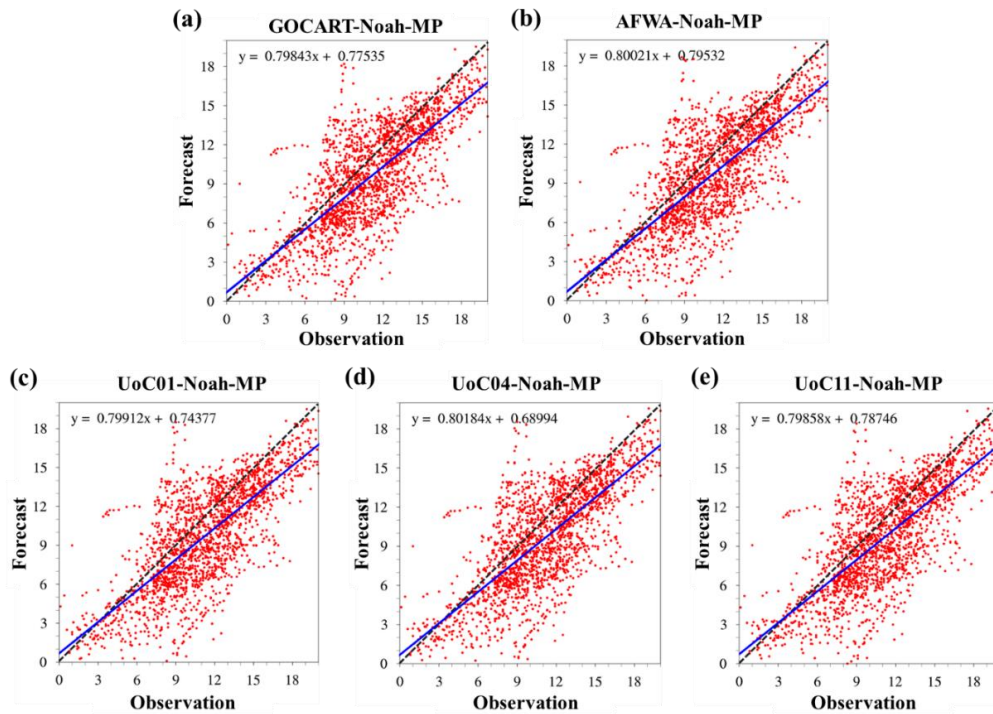


Figure 5: Scatter plots showing the relationship between observed and forecasted values for T2m, using Noah-MP-based combinations. Each panel represents a different scheme combinations: (a) GOCART-Noah-MP, (b) AFWA-Noah-MP, (c) UoC01-Noah-MP, (d) UoC04-Noah-MP, and (e) UoC11-Noah-MP. The black dashed line represents that the forecast perfectly matches the observation. The blue line indicates the linear regression fits the data, providing relationship between the observed and forecasted values.

(Revised manuscript)

Figure 5 shows the scatter plot of WS10m for UoC04-based combinations. In these combinations, the simulated values exhibited a clear tendency to overestimate compared to the observed values. Notably, UoC04-Noah-MP, which showed the best performance in WS10m validation based on MBE and RMSE, had the smallest intercept, indicating the lowest systematic bias among the four scheme combinations, followed by UoC04-RUC, UoC04-CLM4, and UoC04-Noah. Similar results were observed for T2m and RH2m (not shown). This finding aligns with the validation of meteorological variables, where Noah-MP-based combinations demonstrated the best performance.

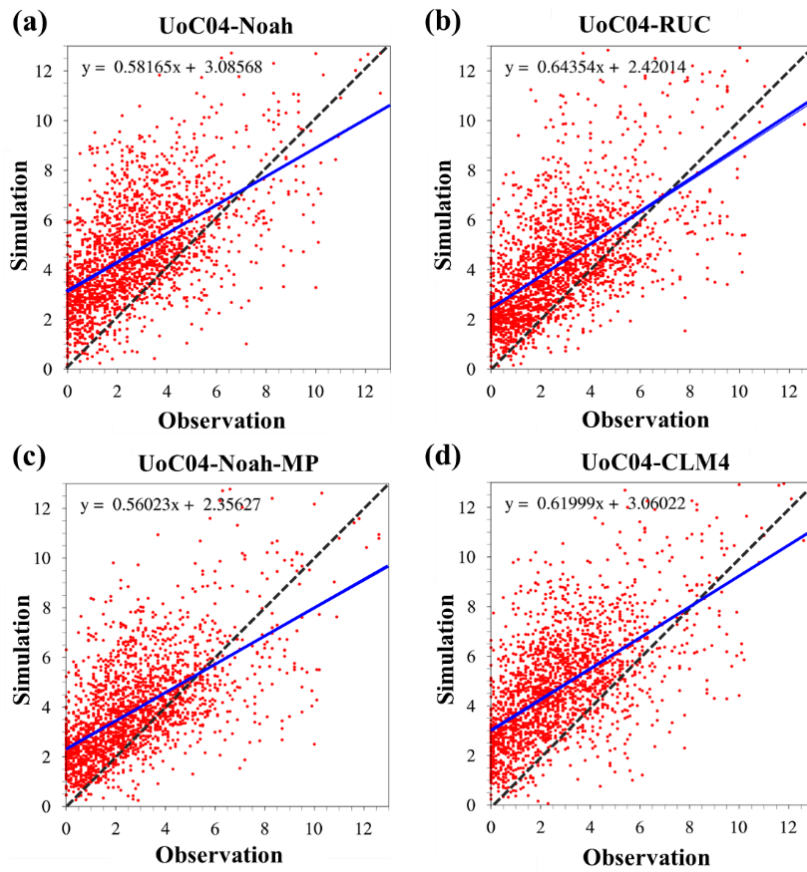


Figure 5: Scatter plots showing the relationship between observed and simulated values for WS10m, using UoC04-based combinations. Each panel represents a different scheme combination: (a) UoC04-Noah, (b) UoC04-RUC, (c) UoC04-Noah-MP, and (d) UoC04-CLM4. The black dashed line represents that the simulation perfectly matches the observation. The blue line indicates the linear regression fits the data, providing a relationship between the observed and simulated values.